

NRC Publications Archive Archives des publications du CNRC

Effects of geometry variations on the performance of podded propulsors

Islam, M.; Veitch, B.; Molloy, S.; Bose, N.; Liu, P.

This publication could be one of several versions: author's original, accepted manuscript or the publisher's version. / La version de cette publication peut être l'une des suivantes : la version prépublication de l'auteur, la version acceptée du manuscrit ou la version de l'éditeur.

Publisher's version / Version de l'éditeur:

SNAME Maritime Technology Conference & Expo and Ship Production Symposium [Proceedings], 2007

NRC Publications Archive Record / Notice des Archives des publications du CNRC :

<https://nrc-publications.canada.ca/eng/view/object/?id=97bbefc2-edcd-4ce7-9dcc-79f201702830>

<https://publications-cnrc.canada.ca/fra/voir/objet/?id=97bbefc2-edcd-4ce7-9dcc-79f201702830>

Access and use of this website and the material on it are subject to the Terms and Conditions set forth at

<https://nrc-publications.canada.ca/eng/copyright>

READ THESE TERMS AND CONDITIONS CAREFULLY BEFORE USING THIS WEBSITE.

L'accès à ce site Web et l'utilisation de son contenu sont assujettis aux conditions présentées dans le site

<https://publications-cnrc.canada.ca/fra/droits>

LISEZ CES CONDITIONS ATTENTIVEMENT AVANT D'UTILISER CE SITE WEB.

Questions? Contact the NRC Publications Archive team at

PublicationsArchive-ArchivesPublications@nrc-cnrc.gc.ca. If you wish to email the authors directly, please see the first page of the publication for their contact information.

Vous avez des questions? Nous pouvons vous aider. Pour communiquer directement avec un auteur, consultez la première page de la revue dans laquelle son article a été publié afin de trouver ses coordonnées. Si vous n'arrivez pas à les repérer, communiquez avec nous à PublicationsArchive-ArchivesPublications@nrc-cnrc.gc.ca.

Effects of Geometry Variations on the Performance of Podded Propulsors

Mohammed F. Islam, (SM), Brian Veitch, (M), Susan Molloy, (SM), Neil Bose, (FL), and Pengfei Liu, (M)

This paper presents results and analyses of an experimental study into the effects of geometric parameters on the propulsive characteristics of puller and pusher podded propulsors in straight course open water conditions. Five geometric parameters were chosen for the current study and a design of experiment technique was used to design a series of 16 pods that combined the parameters. Tests on the 16 different pod-strut-propeller combinations in puller and pusher configurations were completed using a custom designed podded propeller test rig. The dynamometry consisted of a six-component global dynamometer and a three-component pod dynamometer. The test rig was used to measure the thrust and torque of the propellers, and forces and moments on the whole unit in the three orthogonal directions. The design of experiment analysis technique was then used to identify the most significant geometric parameters and interaction of parameters that affect propeller thrust, torque and efficiency as well as unit thrust and efficiency in both the puller and pusher configurations. An uncertainty analysis of the measurements is also presented.

KEY WORDS: Podded propulsors; puller and pusher propulsors; pod geometry variation; propulsive performance; design of experiments;

INTRODUCTION

Podded propulsors have become attractive to the cruise, ferry and other shipping sectors. The geometry variations of the pod that encases the motor and shaft of a podded propulsor have been guided primarily by the size of available motors. In their study on podded propulsor optimization, Goubault and P  r  e (2004) concluded that the pod motor parameters are not as influential on the hydrodynamic performance as the geometric parameters. This emphasizes the need for further research on pod-strut shape to better understand the effect of geometry on podded propulsors' hydrodynamic performance. Karafiath and Lyons (1998) presented a study on the effect of pod geometry on the performance of podded propulsors. Pod length and strut position were varied using four pods to study their effects on pod drag and pod-propeller interactions.

As motor design becomes more flexible, the relationship between various geometric parameters and performance becomes an important design consideration. The determination of the geometric parameters needs to be supported by detailed investigations into their individual and their combined (interaction) effects on the hydrodynamic performance of the propulsor. There are a number of geometric parameters that can be used to optimize the design of a pod and five were chosen for the current study, specifically, pod diameter, pod length and taper length, strut distance from the propeller plane, and propeller hub taper angle. Our study focuses on the effects of geometry variations on the hydrodynamic performance of both puller and pusher podded propulsors. It is important to study the performance of pusher and puller propulsors separately because of the necessary different flow conditions involved.

This research program on podded propellers is being undertaken jointly by the Ocean Engineering Research Centre (OERC) at

Memorial University of Newfoundland (MUN) and the National Research Council's Institute for Ocean Technology (IOT), with the support of Oceanic Consulting Corporation, and Thordon Bearings Ltd. The program combines parallel developments in numerical prediction methods and experimental evaluation. Amongst the hydrodynamic issues that have been identified are questions regarding the effects of hub taper angle (Islam, 2004; Islam *et al.*, 2004; Islam *et al.*, 2005; Taylor *et al.*, 2005 and Taylor, 2005), pod-strut configuration (Islam, 2004 and Taylor, 2005), pod-strut interactions (He *et al.*, 2005a and He *et al.*, 2005b), gap pressure (MacNeill *et al.*, 2004), and pod-strut geometry (Molloy *et al.*, 2005) on podded propeller performance.

THE GEOMETRIC SERIES AND EXPERIMENTAL APPARATUS

Using existing commercial pods as a baseline, five geometric parameters were selected that allowed variation in the primary dimensions of the pod-strut-propeller hub (Molloy *et al.*, 2005). The pod length, diameter and taper length, as well as strut distance from the propeller plane, and propeller hub taper angle were chosen as key defining parameters of the propulsor (Fig. 1). Values of these parameters were chosen so that there was one set of parameters in the series that is higher than the average commercial dimensions and one set lower. The high and low values of the parameters (Table 1) were then combined to give a series of 16 pods based on a fractional factorial design of experiment technique (Molloy, 2003). Two propellers with hub taper angles of -15° and -20° (denoted as Pull- 15° and Pull- 20° , respectively) were used with the pod series in puller configuration, and two propellers with hub taper angles of 15° and 20° (denoted as Push+ 15° and Push+ 20° , respectively) were used with the pod series in pusher configuration. These four propellers had the same blade sectional geometry but different hub taper angles. Details of the geometry of the propellers can be found in (Liu, 2006).

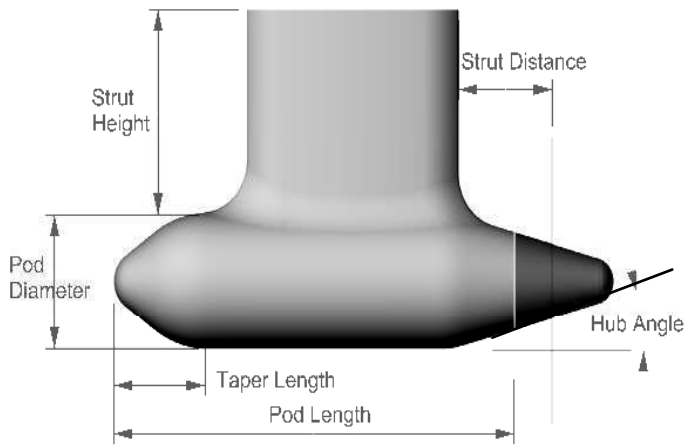


Table 1. High and low values of the geometric parameters of the pod models.

External Dimensions of Model Pod	Avg. Values mm	Low Values mm	High Values mm
Propeller Diameter,	270	270	270
Pod Diameter, D_{Pod}	139	128	166
Pod Length, L_{Pod}	430	430	524
Strut Distance, S_{Dist}	100	75	133
Taper Length, TL	110	69	150
Hub Angle, H_{Angle}	15° & 20°	15°	20°

Fig. 1. Geometric parameters used to define pod-strut geometry.

For the research work, 16 combinations of dimensions were designed and manufactured as listed in Table 2. The pod combinations were selected to include one combination with all dimensions low and one with all dimensions high, denoted as Pod 1 and Pod 16. The list of symbols of the parameters used in the paper is shown in Table 2. The physical models of the 16 pods tested in the geometric series are shown in Fig. 2.

Table 2. Combinations of dimensions of the 16 pods (used in fractional factorial design). Here, A is the ratio of pod diameter to propeller diameter, D_{Pod}/D_{Prop} , B is the ratio of pod length to propeller diameter, L_{Pod}/D_{Prop} , C is the ratio of pod taper length to propeller diameter, TL/D_{Prop} , D is the ratio of strut distance to propeller diameter, S_{Dist}/D_{Prop} , and E is the propeller hub taper angle, H_{Angle} .

Pod No.	Factor A D_{Pod}/D_{Prop}	Factor B L_{Pod}/D_{Prop}	Factor C TL/D_{Prop}	Factor D S_{Dist}/D_{Prop}	Factor E H_{Angle}
Ratios are based on propeller diameter, D_{Prop} of 270 mm					
Pod 1	0.474	1.593	0.256	0.370	15
Pod 2	0.474	1.593	0.256	0.489	20
Pod 3	0.474	1.593	0.556	0.489	15
Pod 4	0.474	1.593	0.556	0.370	20
Pod 5	0.474	1.941	0.256	0.370	20
Pod 6	0.474	1.941	0.256	0.489	15
Pod 7	0.474	1.941	0.556	0.370	15
Pod 8	0.474	1.941	0.556	0.489	20
Pod 9	0.615	1.593	0.256	0.370	15
Pod 10	0.615	1.593	0.256	0.489	20
Pod 11	0.615	1.593	0.556	0.370	20
Pod 12	0.615	1.593	0.556	0.489	15
Pod 13	0.615	1.941	0.256	0.370	20
Pod 14	0.615	1.941	0.256	0.489	15
Pod 15	0.615	1.941	0.556	0.370	15
Pod 16	0.615	1.941	0.556	0.489	20

The pod series tests used a fractional factorial design technique, a method of experimentation used to examine the effects of single parameters and interactions between parameters for multifactor experiments. In factorial experiment designs, a factor is a major independent variable. In this method, the

significance of individual factors is ranked in an ascending order based on the estimate of their effects on the overall result of the experiments. An experimenter can go through the process of logical elimination of insignificant factors and rerun the tests using only the most influential factors, thus making the

experimentation simpler. Some factors or interaction factors are aliased with each other and cannot be differentiated (Montgomery, 2005). The details of the factorial effect aliases in our test series design can be found in (Islam, 2004). The factorial analysis was used to determine which geometric

parameters of a pod-strut-propeller have the most significant effect on the measured performance values (of propeller and unit thrust, propeller torque, propeller and unit efficiency) in an open water propulsion unit test in puller and pusher configurations.

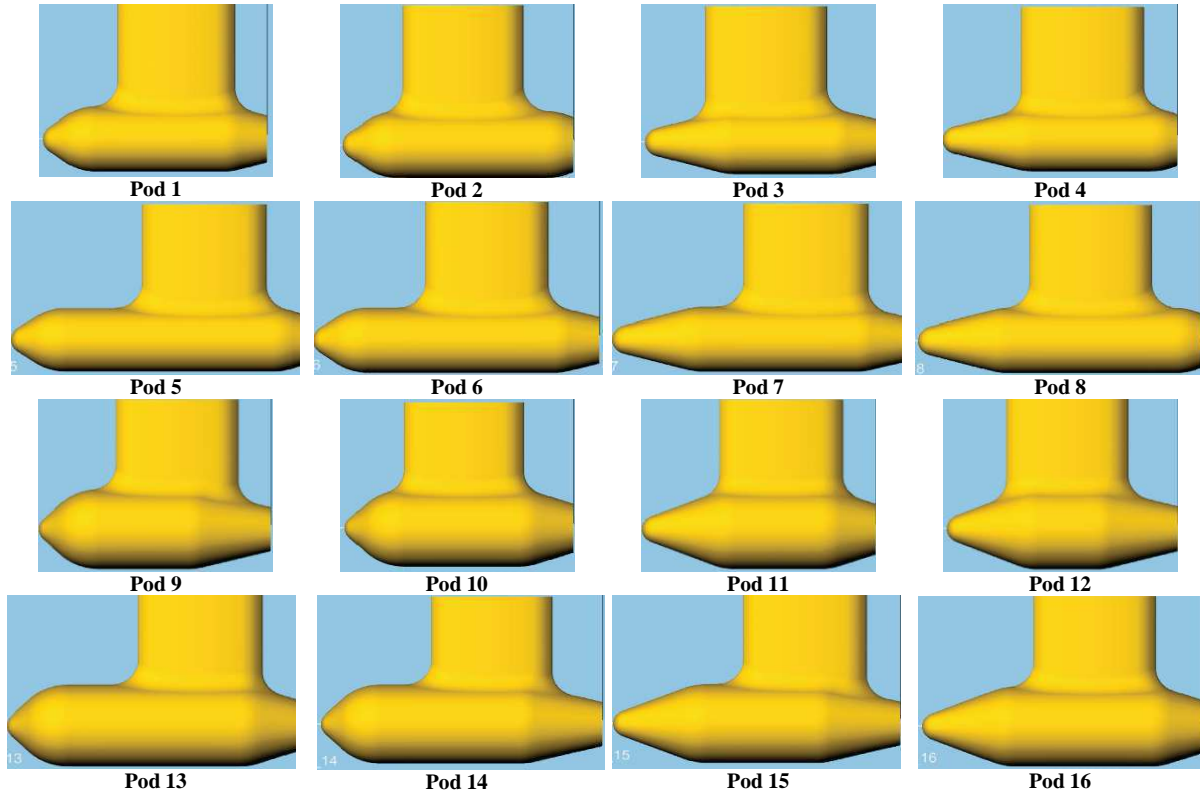


Fig. 2. Geometric models of the pod series used in the experiments.

The open water tests of the 16 pods were performed in accordance with the ITTC recommended procedure (2002a) and the description provided in Mewis (2001). A custom-designed dynamometer system was used to measure propeller thrust, torque and unit thrust of the pod series in both puller and pusher configurations. A motor was fitted above the propeller boat to drive the propeller via a belt system. The center of the propeller shaft was $1.5D_{Prop}$ below the water surface. The part of the shaft above the strut went through the boat. The propeller boat stayed 3 to 5 mm above the water surface to avoid waves caused by the strut piercing the surface. Water temperature, carriage speed, V_A , and the rotational speed of the propeller, n , were measured. Details of the experimental apparatus can be found in MacNeill *et al.* (2004).

RESULTS AND ANALYSIS

The dynamometer system measured propeller and pod forces and moments as follows: propeller thrust at the propeller end (T_{Prop}), propeller thrust at the pod end (T_{Pod}), propeller torque (Q), unit longitudinal force (T_{Unit} or F_X), unit transverse force (F_Y) and unit vertical force (F_Z). Two thrust load cells were used to measure propeller thrust at the two ends of the propeller shaft (T_{Prop} and T_{Pod}). The difference between the two measurements was insignificant taking into account the uncertainty in the system. In the current paper, only the propeller thrust at the

propeller end (T_{Prop}) is presented. The experimental results were analyzed in terms of propeller thrust coefficient, K_{TProp} , propeller torque coefficient, $10K_Q$, propulsive efficiency, η_{Prop} , unit thrust coefficient, K_{TUnit} , and unit efficiency, η_{Unit} , all versus propeller advance coefficient, J . K_{TProp} , K_Q , η_{Prop} , K_{TUnit} , η_{Unit} and J are defined in equations 1-6, respectively. Additional experiments were conducted to study *Reynolds Number* effects on the puller and pusher propulsors' performance (Islam, 2006a). The study showed that the *Reynolds Number* effects became negligible at rotational speeds of 11 (equivalent to $Re=6.50 \times 10^5$) and above, as both the propeller thrust and unit thrust stabilized at that rotational speed for all advance coefficient values. In all of the tests for pod geometry effects, a constant shaft rotational speed of 11 rps was used. Equations 1 to 6 were used to present the measurements.

$$K_{TProp} = T_{Prop} / (\rho n^2 D^4) \quad (1)$$

$$K_Q = Q / (\rho n^2 D^5) \quad (2)$$

$$\eta_{Prop} = [J / (2\pi)] \times (K_{TProp} / K_Q) \quad (3)$$

$$K_{TUnit} = T_{Unit} / (\rho n^2 D^4) \quad (4)$$

$$\eta_{Unit} = [J / (2\pi)] \times (K_{TUnit} / K_Q) \quad (5)$$

$$J = V_A / (nD) \quad (6)$$

EXPERIMENTAL RESULTS

Pod Series in Puller Configuration

The propeller thrust coefficient, K_{TProp} , propeller torque coefficient, $10K_Q$ and propulsive efficiency, η_{Prop} values for each of the 16 pods in the puller pod series experiments (in the range of $J=0.0\sim 1.20$) are presented in Figs. 3, 4 and 5, respectively. The tests were conducted at 17 different advance coefficients with repeated tests at 4 advance coefficients. Tables A-1 and A-2 present the K_{TProp} and $10K_Q$ values, respectively, for the pods in puller configuration.

With reference to the Figures, for the puller propulsors in the series, the K_{TProp} values at $J = 0$ of the 16 pods ranged from 0.464-0.495, an approximately 7% spread based on the lowest K_{TProp} given by pod 15. At $J = 0.8$, the K_{TProp} values covered 0.152-0.179 (approximately 17% spread based on the lowest K_{TProp}). At $J=0.8$, the highest K_{TProp} was given by pod 16 and the lowest K_{TProp} was given by pod 3. The torque coefficient ($10K_Q$) values of the different pods ranged from 0.679-0.692 (approximately 2% spread based on the lowest $10K_Q$ given by pod 3) at $J = 0$ and 0.275-0.312 (approximately 14% spread based on the lowest $10K_Q$ given by pod 4) at $J = 0.8$. The η_{Prop} values of the different pods ranged from 0.647-0.753 at $J = 0.8$ and 0.625-0.824 at $J = 1.0$. The trends showed that for puller configuration propulsors, there was significant variation in K_{TProp} , $10K_Q$ and η_{Prop} values with the change of the geometric parameters. At $J=0$, the thrust coefficients of the pods 1, 3, 6, 7, 12, 14, 15 were lower than those of pod 9 and the thrust coefficients of the remaining pods were higher than those of pod 9. At $J=0.8$, the propulsive efficiencies of the pods 1, 3, 6, 7, 12, 14, 15 were lower than those of pod 9 and the propulsive efficiencies of the remaining pods were higher than those of pod 9. This indicated that the efficiency of the propeller attached to pod 9 was approximately the average of all the other pods. Among the pods, pod 3 had the lowest efficiency ($\eta_{Prop}=0.647$) and pod 16 had the highest efficiency ($\eta_{Prop}=0.753$) at the design advance coefficient of $J=0.8$.

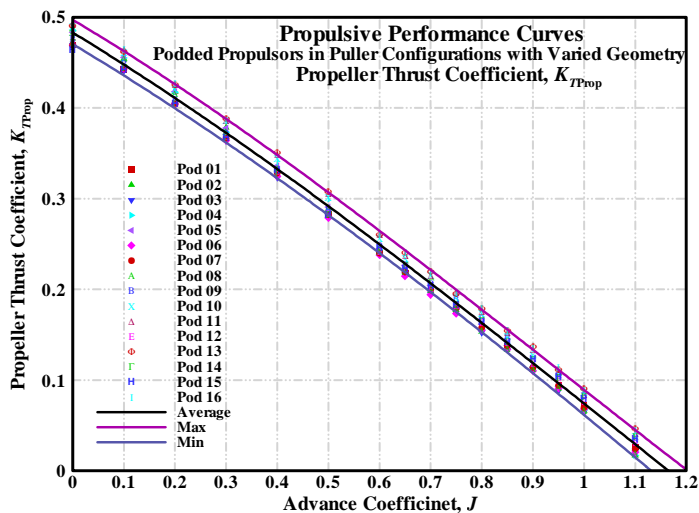


Fig. 3. Experimental results: Propeller thrust coefficient of all 16 puller pods in the series.

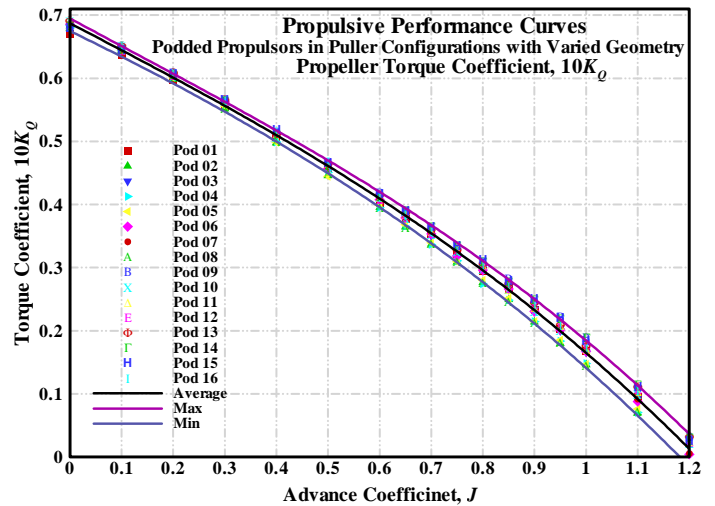


Fig. 4. Experimental results: Torque coefficient of all 16 puller pods in the series.

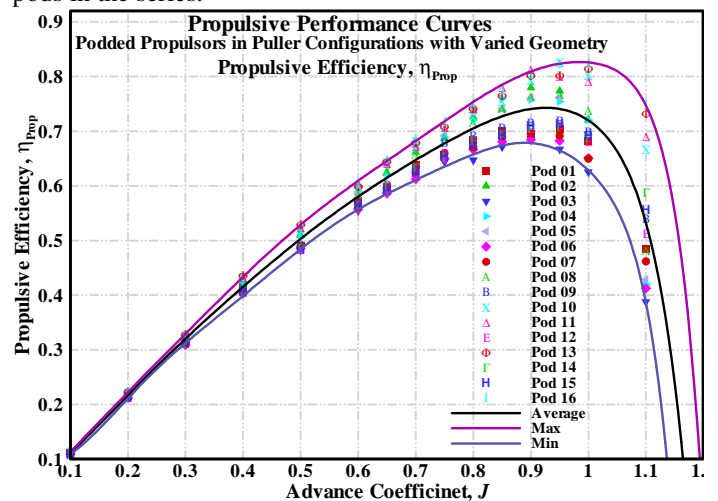


Fig. 5. Experimental results: Propeller efficiency of all 16 puller pods in the series.

The unit thrust coefficient, K_{TUnit} and unit efficiency, η_{Unit} values for each of the 16 pods in the pod series experiments (in the range of $J=0.0\sim 1.20$) are presented in Figs. 6 and 7. The unit thrust coefficient values at $J = 0$ for the different pods ranged from 0.458 to 0.484, an approximately 6% spread based on the lowest K_{TUnit} given by pod 7. At $J = 0.8$, the K_{TUnit} values ranged from 0.13 and 0.153, an approximately 18% spread based on the lowest K_{TUnit} given by pod 4. The η_{Unit} values of the different pods ranged from 0.564 to 0.645 at $J = 0.8$ and from 0.366 to 0.565 at $J = 1.0$. The trends showed that there is significant variation in K_{TUnit} and η_{Unit} values with the change of the geometric parameters. At $J=0$, the thrust coefficients of the pods 1, 3, 6, 7, 12, 14, 15 were lower than those of pod 9 and the thrust coefficients of the remaining pods were higher than those of pod 9. Among these pods, pod 9 had the lowest unit efficiency ($\eta_{Unit}=0.565$) and pod 5 had the highest unit efficiency ($\eta_{Unit}=0.645$) at the design advance coefficient of $J=0.8$. Table A-3 presents the K_{TUnit} values for the pods in puller configuration.

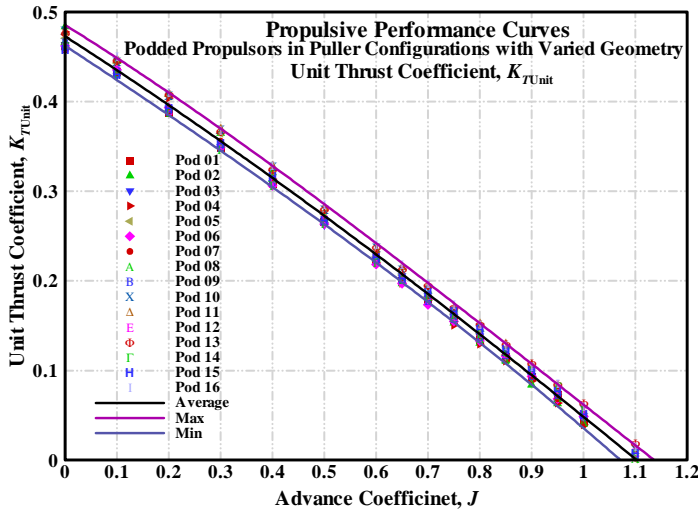


Fig. 6. Experimental results: Unit thrust coefficient of all 16 puller pods in the series.

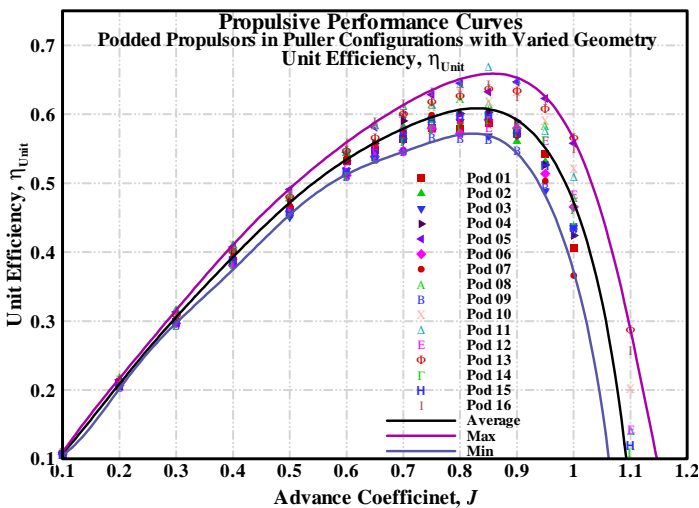


Fig. 7. Experimental results: Unit propulsive efficiency of all 16 puller pods in the series.

Pod Series in Pusher Configuration

The propeller thrust coefficient, K_{TProp} , propeller torque coefficient, $10K_Q$ and propulsive efficiency, η_{Prop} values for each of the 16 pods in the pusher pod series experiments (in the range of $J=0.0\sim 1.20$) are presented in Figs. 8, 9 and 10, respectively. The tests were conducted at 17 different advance coefficients. Tests were repeated at a minimum of 4 advance coefficients. Table A-4 and A-5 present the K_{TProp} and $10K_Q$ values for the pods in pusher configurations, respectively.

For the pusher propulsors in the series, the K_{TProp} values at $J = 0$ of the 16 pods ranged from 0.4564 to 0.4715, an approximately 4% spread based on the lowest K_{TProp} given by pod 7. At $J = 0.8$, the K_{TProp} values were in a range of 0.1469-0.1724 (approximately 17% spread based on the lowest K_{TProp}). At $J=0.8$, the highest K_{TProp} was given by pod 4 and the lowest K_{TProp} was given by pod 13. The torque coefficient ($10K_Q$) values of the different pods ranged from 0.6532 to 0.6852 (approximately 5% spread based on the lowest $10K_Q$ given by

pod 12) at $J = 0$, and from 0.275 to 0.312 (approximately 14% spread based on the lowest $10K_Q$ given by pod 1) at $J = 0.8$. The η_{Prop} values of the different pods ranged from 0.666-0.712 at $J = 0.8$ and 0.580-0.702 at $J = 1.0$. The trends showed that for the pusher configuration propulsors, there was significant variation in K_{TProp} , $10K_Q$ and η_{Prop} values with changes of the geometric parameters. At $J=0$, the thrust coefficients of the pods 2, 7, 8, 12, 13, 14 were lower than those of pod 9 and the thrust coefficients of the remaining pods were higher than those of pod 9. At $J=0.8$, the propulsive efficiencies of the pods 5, 7, 9, 13, 14, 15, 16 were lower than those of pod 8 and the propulsive efficiencies of the remaining pods were higher than those of pod 8. This indicated that the efficiency of the propeller attached with pod 8 was approximately the average of all the other pods. Among the pods, pod 13 had the lowest efficiency ($\eta_{Prop} = 0.666$) and pod 12 had the highest efficiency ($\eta_{Prop} = 0.712$) at the design advance coefficient of $J=0.8$.

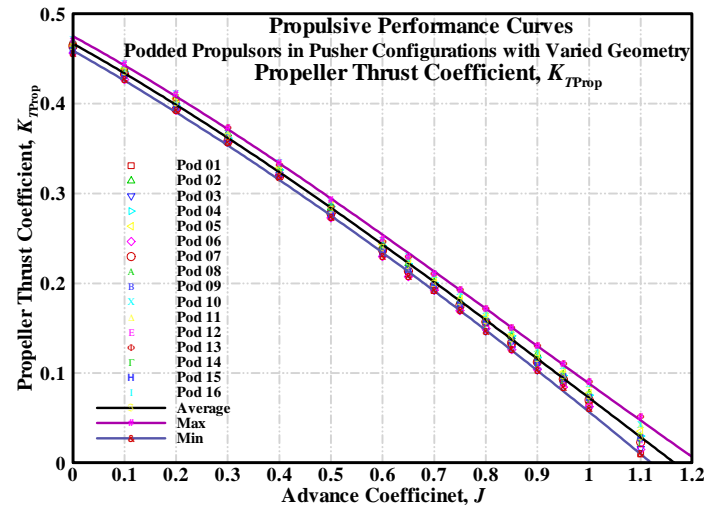


Fig. 8. Experimental results: Propeller thrust coefficient of all 16 pusher pods in the series.

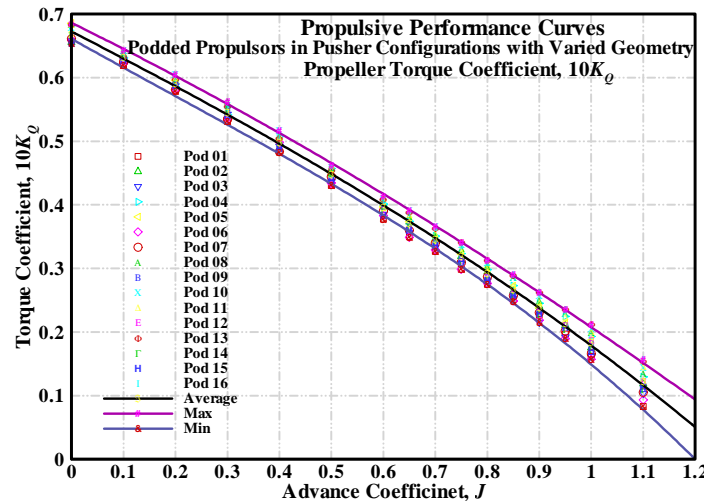


Fig. 9. Experimental results: Torque coefficient of all 16 pusher pods in the series.

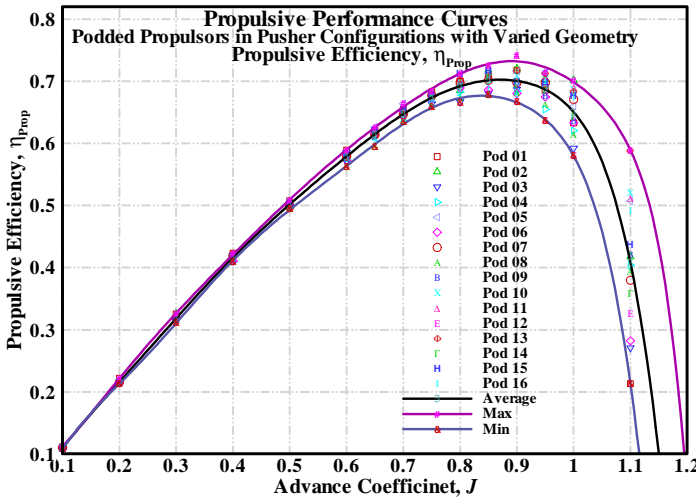


Fig. 10. Experimental results: Propeller efficiency of all 16 pusher pods in the series.

The K_{TUnit} and η_{Unit} values for each of the 16 pods in the pusher pod series experiments (in the range of $J=0.0\sim 1.20$) are presented in Figs. 11 and 12, respectively. The unit thrust coefficient (K_{TUnit}) values at $J = 0$ of the different pods ranged from 0.440-0.462, an approximately 5% spread based on the lowest K_{TUnit} given by pod 1. At $J = 0.8$, the K_{TUnit} values cover a ranged of 0.112-0.143 (approximately 18% spread based on the lowest K_{TUnit} given by pod 12). The η_{Unit} values of the different pods ranged from 0.514-0.634 at $J = 0.8$ and 0.232-0.415 at $J = 1.0$. The trends showed that there was significant variation in K_{TUnit} and η_{Unit} values with the change of the geometric parameters. At $J=0$, the unit thrust coefficients of the pods 1, 3, 4, 5, 6, 8, 16 were lower than those of pod 9 and the thrust coefficients of the remaining pods were higher than those of pod 9. Among the pods, pod 4 had the lowest unit efficiency ($\eta_{Unit}=0.514$) and pod 11 had the highest unit efficiency ($\eta_{Unit}=0.634$) at the design advance coefficient of $J=0.8$. Table A-6 presents the K_{TUnit} values for the pods in pusher configuration.

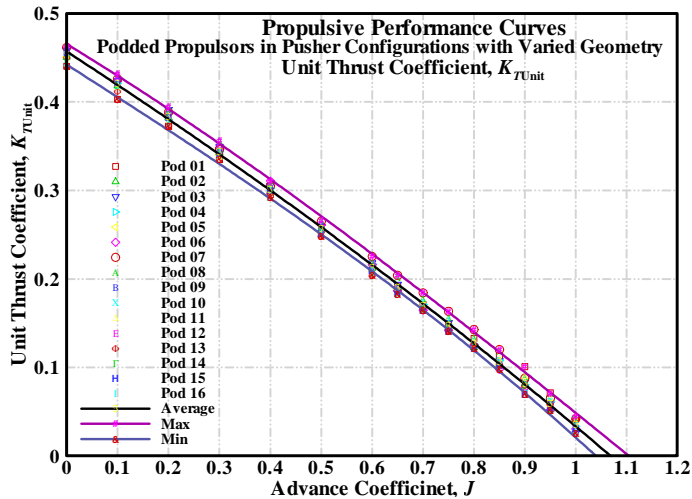


Fig. 11. Experimental results: Unit thrust coefficient of all 16 pusher pods in the series.

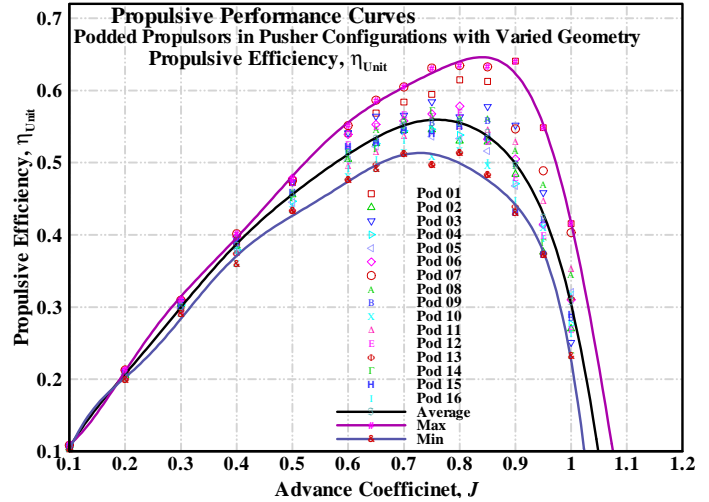


Fig. 12. Experimental results: Unit propulsive efficiency of 16 pusher pods in the series.

UNCERTAINTY ANALYSIS

While the details of uncertainty analysis are beyond the scope of this paper, a brief discussion of the levels of uncertainty in the above results is given below. To assess the uncertainty in each set of experiments and to identify the major factors influencing these results, a thorough uncertainty analysis was conducted (Islam, 2006b). The techniques used were based on adaptations of uncertainty analysis techniques outlined in ITTC recommended Procedure (2002b); Bose and Luznik (1996); Coleman and Steele (1989) and Hess *et al.* (2000).

The overall uncertainty in the non-dimensional performance coefficients of the podded propulsors required proper identification of all the variables contained within the data reduction expressions (equations 1-6). The experimental approaches used to obtain the data for each of the variables in the expressions were influenced by a variety of elemental sources of error. These elemental sources were estimated, and combined using the root-sum-square (RSS) method to give the bias and precision limits for each of the variables. The bias errors consisted of many elemental sources of error, which depended on the approaches followed to measure the variables. However, for the precision error estimates of most variables, only one source of error (repeatability) was considered significant. In order to calculate the uncertainty due to calibration of the six-component dynamometer measurement, it was required to determine how the uncertainties in the calibration data propagates into each element of the interaction matrix and into the measured forces and moments (Hess *et al.*, 2000).

The error estimates used in the determination of the bias and precision errors in this study were considered to be 95% coverage estimates. The bias uncertainty and the precision uncertainty were combined using the root-sum-square (RSS) method to provide estimates of overall uncertainty levels in these variables. The overall uncertainty was thus considered to be a 95% coverage estimate.

The final step in the methodology of uncertainty analysis was to determine how uncertainties in each of the variables propagate through the data reduction equations. Using the approaches described in Bose and Luznik (1996) and Coleman and Steele (1989), the uncertainty expressions for each set of experiments were developed as shown in equation 7 to 10, where U denotes

$$\left(\frac{U_{K_{TProp}}}{K_{TProp}}\right)^2 = \left(\frac{U_{TProp}}{T_{Prop}}\right)^2 + \left(\frac{U_{\rho}}{\rho}\right)^2 + 4\left(\frac{U_n}{n}\right)^2 + 16\left(\frac{U_D}{D}\right)^2 \quad (7)$$

$$\left(\frac{U_{K_Q}}{K_Q}\right)^2 = \left(\frac{U_Q}{Q}\right)^2 + \left(\frac{U_{\rho}}{\rho}\right)^2 + 4\left(\frac{U_n}{n}\right)^2 + 25\left(\frac{U_D}{D}\right)^2 \quad (8)$$

$$\left(\frac{U_{K_{TUnit}}}{K_{TUnit}}\right)^2 = \left(\frac{U_{TUnit}}{T_{Unit}}\right)^2 + \left(\frac{U_{\rho}}{\rho}\right)^2 + 4\left(\frac{U_n}{n}\right)^2 + 16\left(\frac{U_D}{D}\right)^2 \quad (9)$$

$$\left(\frac{U_J}{J}\right)^2 = \left(\frac{U_{V_A}}{V_A}\right)^2 + \left(\frac{U_n}{n}\right)^2 + \left(\frac{U_D}{D}\right)^2 \quad (10)$$

the uncertainties in the corresponding coefficients denoted by the subscripts. It is to be noted that, in deriving the expressions, the cross-correlated bias limits (Coleman and Steele, 1989) were ignored. Strictly they should have been included, but they would have, in the current case, reduced the total uncertainty.

In the expressions for the podded propulsors' tests, it should be noted that for both thrust and torque coefficient uncertainties, the tare thrust and frictional torque were imbedded in the corresponding measurements. Since the tare thrust and frictional torque were part of the same data stream as the thrust and torque readings, they were not treated as an independent contributor of

error to the corresponding coefficients, but rather as a bias error on the static-zero value of the thrust and the torque measurements. The resulting error estimates for the podded propulsor tests are given in Table 3 below.

Table 3. Uncertainty in the measurements of the pod series data.

J	U_J (+/-)	U_J/J (+/-)	$U_{K_{TProp}}$ (+/-)	$U_{K_{TProp}}/K_{TProp}$ (+/-)	U_{K_Q} (+/-)	U_{K_Q}/K_Q (+/-)	$U_{K_{TUnit}}$ (+/-)	$U_{K_{TUnit}}/K_{TUnit}$ (+/-)
0.00	-	-	5.78E-03	1.21	7.61E-03	1.11	4.75E-03	1.01
0.10	5.20E-03	5.20	5.59E-03	1.24	7.57E-03	1.17	4.39E-03	1.00
0.20	5.27E-03	2.63	5.28E-03	1.28	7.25E-03	1.20	4.05E-03	1.02
0.30	5.37E-03	1.79	5.02E-03	1.34	6.68E-03	1.19	3.74E-03	1.05
0.40	5.52E-03	1.38	4.74E-03	1.42	6.27E-03	1.23	3.40E-03	1.08
0.50	5.70E-03	1.14	4.62E-03	1.60	5.90E-03	1.28	3.07E-03	1.13
0.60	5.90E-03	0.98	4.22E-03	1.71	5.92E-03	1.45	2.66E-03	1.17
0.70	6.15E-03	0.88	4.02E-03	1.96	5.18E-03	1.47	2.44E-03	1.33
0.80	6.40E-03	0.80	3.33E-03	2.03	5.30E-03	1.79	2.22E-03	1.71
0.90	6.71E-03	0.75	2.89E-03	2.40	4.66E-03	2.00	2.21E-03	2.30
1.00	7.02E-03	0.70	2.43E-03	3.21	4.94E-03	2.94	1.43E-03	2.86
1.10	7.32E-03	0.67	1.43E-03	4.85	4.15E-03	4.38	9.99E-04	2.80
1.20	7.67E-03	0.64	-2.26E-03	12.58	3.82E-03	45.91	-1.34E-03	2.70

Applying the uncertainty limits to the performance curves of pod 16 in the form of error bars yields a plot as shown in Fig. 13. From the figure, it is observed that the curves fitted to the data lie inside the error bars. Therefore, the fitted curves provide a good representation of the trends indicated by the results.

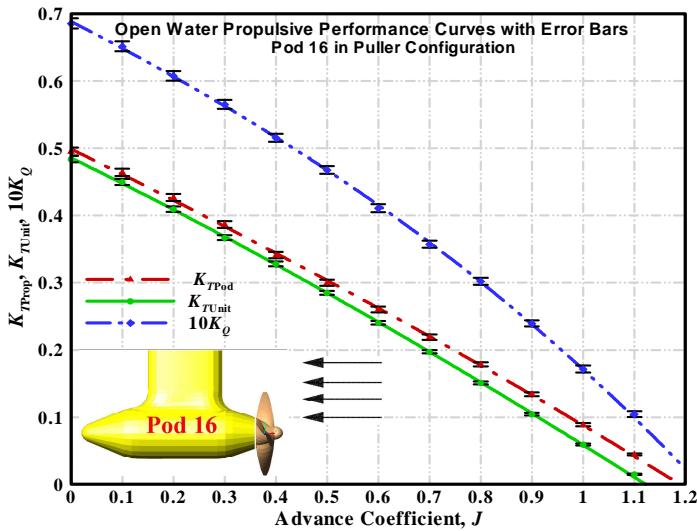


Fig. 13. Propulsive performance of pod 16 in puller configuration with error bars.

DOE ANALYSIS

The design of experiment data analysis was completed using the commercial software, Design Expert® (2005). The software allows the user to choose a factorial design that meets specific research configuration requirements; in this case the design includes one pod with all-low factors and one pod with all-high factors. The analysis of the data using a fractional factorial design technique resulted in the identification of the most significant factors and interactions of factors that affect the propulsive performance of the podded propulsors both in puller and pusher configurations.

DOE Analysis of Puller Propulsors

The Analysis of Variance Approach (ANOVA, see Montgomery, 2005) incorporating with a 95% confidence

interval was used to examine the geometric parameters of the series that have the most significant impact on the performance of the podded propulsors. A separate analysis was completed for each advance coefficient. Table 4 lists all the factors and interactions of factors that have significant influence on the performance coefficients: propeller thrust coefficient, K_{TProp} , propeller torque coefficient, K_Q , propeller efficiency, η_{Prop} , unit thrust coefficient, K_{TUnit} and unit efficiency, η_{Unit} for the puller propulsors in the pod series. The factors are designated as shown in Table 2. Table 4 shows that the significant factors that come up repeatedly over the range of J values are A (the ratio of pod diameter to propeller diameter, D_{Pod}/D_{Prop}), D (the ratio of strut distance to propeller diameter, S_{Dist}/D_{Prop}), E (hub taper angle, H_{Angle}), AE (interaction of D_{Pod}/D_{Prop} and H_{Angle}) and BD (interaction of L_{Pod}/D_{Prop} and S_{Dist}/D_{Prop}). The factor C (the ratio of pod taper length to propeller diameter, TL/D_{Prop}) did not show any significant influence on the performance coefficients at any advance coefficient.

The factors H_{Angle} and D_{Pod}/D_{Prop} had significant impact on propeller thrust coefficient (K_{TProp}), unit thrust coefficient (K_{TUnit}) and torque coefficient (K_Q) for almost all values of advance coefficients, but as the value of advance coefficient increased from 0, interaction of D_{Pod}/D_{Prop} and H_{Angle} became as significant as the single factors D_{Pod}/D_{Prop} and H_{Angle} (in the range of $J=0.3\sim 1.0$). The factor B (L_{Pod}/D_{Prop}) appeared to have significant effect in the form of interaction with D (S_{Dist}/D_{Prop}) on K_{TUnit} at high values of J (in the range of $J=0.75\sim 0.95$). The factor D (S_{Dist}/D_{Prop}) appeared to have significant effect on K_{TProp} and K_Q at moderate advance coefficients, as shown in Table 4. The propeller and unit efficiencies, η_{Prop} and η_{Unit} were mostly affected by H_{Angle} and D_{Pod}/D_{Prop} ; H_{Angle} being the most influential one at all advance coefficients. D_{Pod}/D_{Prop} played an important role when the advance coefficient was higher than 0.6.

Table 4. Fractional factorial design results: List of significant factors and interaction of factors for puller propulsors. Here, A is the ratio of pod diameter to propeller diameter, D_{Pod}/D_{Prop} , B is the ratio of pod length to propeller diameter, L_{Pod}/D_{Prop} , C is the ratio of pod taper length to propeller diameter, TL/D_{Prop} , D is the ratio of strut distance to propeller diameter, S_{Dist}/D_{Prop} , and E is the propeller hub taper angle, H_{Angle} .

Significant factor and interaction of factors										
J	K_{TProp}		K_{TUnit}		K_Q		η_{Prop}		η_{Unit}	
0.00	A, E		E		A, E		-	-	-	-
0.10	A, E		E		A, E		E		E	
0.20	A, E		E		A, E		E		E	
0.30	A, E	AE	A, E	AE	A, E	AE	E		E	
0.40	A, E	AE	A, E	AE	A, E	AE	E		E	
0.50	A, E	AE	A, E	AE	A, E	AE	E		E	
0.60	A, D, E	AE	A, E	AE	A, D, E	AE	A, E		E	
0.70	A, D, E	AE	A, E	AE	A, D, E	AE	A, E		E	
0.80	A, D, E	AE	A, E	AE, BD	A, D, E	AE	A, E		E	
0.90	A, D, E	AE	A	AE, BD	A, D, E	AE	A, E		A, E	
1.00	A, E		A	BD	A, E		A, E		A, E	
1.10	A, E		A	BD	A, E		A, E	AE	A, E	

As shown in Fig. 14, the parameter D_{Pod}/D_{Prop} had a significant effect on K_{TProp} at $J=0.8$. For a fixed propeller diameter, as the pod diameter increased the K_{TProp} increased. In the puller configuration, the larger pod diameter created larger blockage to the flow behind the propeller. The flow blockage reduced the local inflow velocity, thus the propeller operated at a lower effective advance coefficient, which resulted in increases in the K_{TProp} . The analysis also indicated that the factor A (D_{Pod}/D_{Prop}) was involved in an interaction. This means that while the information in Fig. 14 is valid, there might be indirect impact on K_{TProp} due to the interaction of D_{Pod}/D_{Prop} and H_{Angle} . The parameter A (D_{Pod}/D_{Prop}) had an effect on K_{TUnit} , K_Q , η_{Prop} and η_{Unit} similar to that of K_{TProp} for the advance coefficient values shown in Table 4.

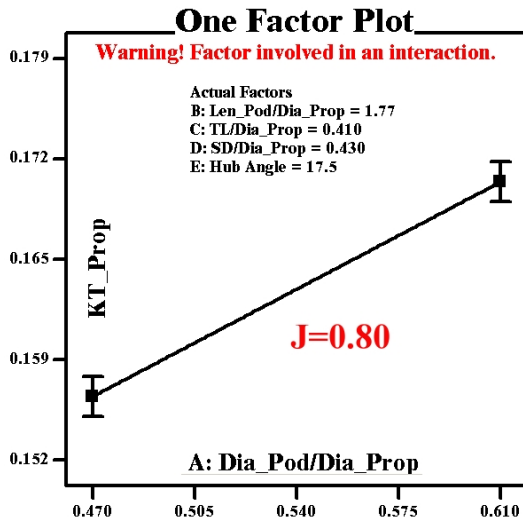


Fig. 14. DOE Analysis: The effect of D_{Pod}/D_{Prop} (A) on propeller thrust at $J=0.8$ for puller propulsors.

tended to decrease slightly because of the blockage effect of the strut. A similar effect was found for K_Q . S_{Dist}/D_{Prop} did not show any effect on K_{TUnit} as an individual factor but had influence on K_{TUnit} as an interaction effect as described later (Fig. 21). Fig. 16 shows the effect of hub angle, E (H_{Angle}) on K_{TProp} . As the hub angle increased, the K_{TProp} also increased. The increasing effect of the hub angle on K_{TProp} was also found in a previous study using the same instrumentation (Islam *et al.*, 2006). Hub angle had a similar effect on K_{TUnit} , η_{Prop} and η_{Unit} . Figs. 17 and 18 show that the parameter hub angle, H_{Angle} , had a significant but opposite effect on K_Q at $J=0$ and $J=0.8$, respectively. As the hub angle increased, the K_Q increased at $J=0$ but decreased at $J=0.8$.

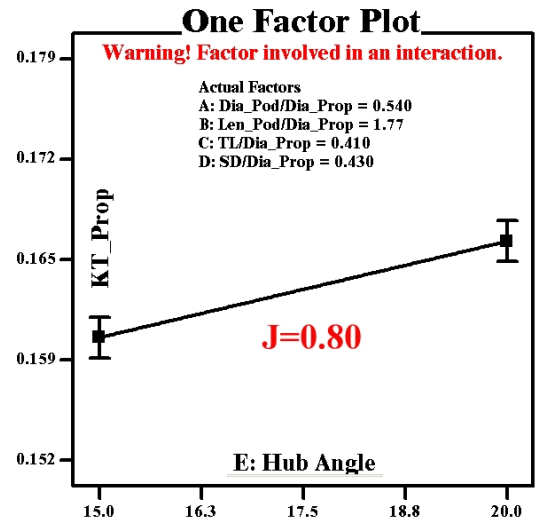


Fig. 16. DOE Analysis: The effect of significant factor, H_{Angle} (E) on propeller thrust at $J=0.8$ for puller propulsors.

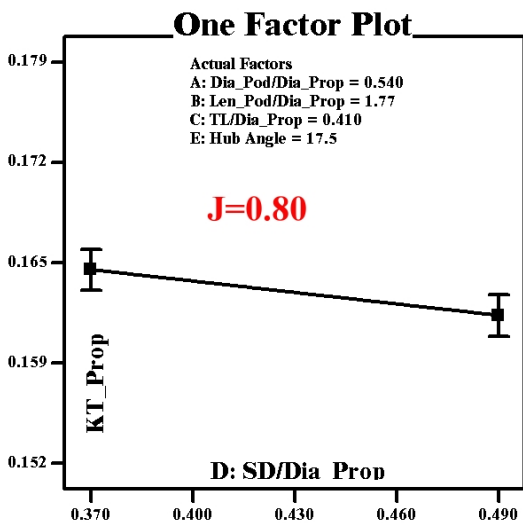


Fig. 15. DOE Analysis: The effect of significant factors, S_{Dist}/D_{Prop} (D) on propeller thrust at $J=0.8$ for puller propulsors.

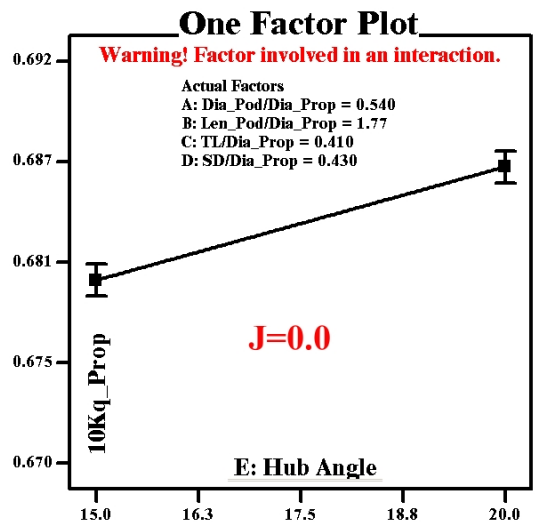


Fig. 17. DOE Analysis: The effect of significant factor, H_{Angle} (E) on propeller torque at $J=0$ for puller propulsors.

Fig. 15 shows the effect of the strut distance, D (S_{Dist}/D_{Prop}) on K_{TProp} ; it shows that as the strut distance increased the K_{TProp}

Fig. 19 shows the interaction effect AE (D_{Pod}/D_{Prop} and H_{Angle}) on K_{TProp} ; it shows that the influence of the factor D_{Pod}/D_{Prop} was more obvious at a high hub angle i.e. increasing the ratio

increased K_{TProp} at a faster rate at high hub angle. When the factor D_{Pod}/D_{Prop} was low, there was little change in K_{TProp} (within 2% based on the lower K_{TProp}) due to change in hub angle. However, when the ratio was high, there was a highly significant effect of hub angle on K_{TProp} (approximately 8% based on the lower K_{TProp}). This indicated that for a fat pod with respect to the propeller (higher value of D_{Pod}/D_{Prop}), the hub angle had more effect on K_{TProp} (as the hub angle increases, the K_{TProp} increases) than a slender pod with a low value of the factor D_{Pod}/D_{Prop} . A similar interaction effect was also found on K_{TUnit} and K_Q .

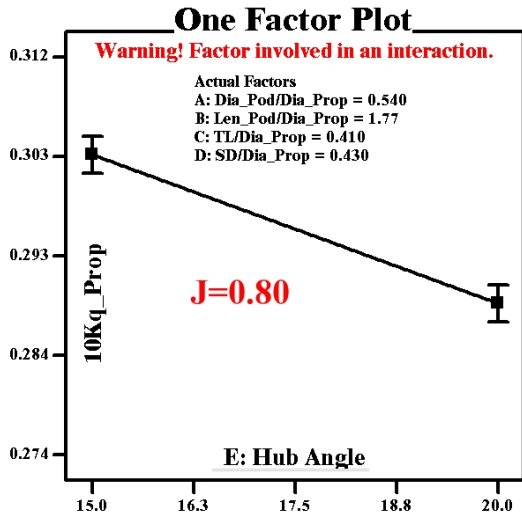


Fig. 18. DOE Analysis: The effect of significant factor, H_{Angle} (E) on propeller torque at $J=0.8$ for puller propulsors.

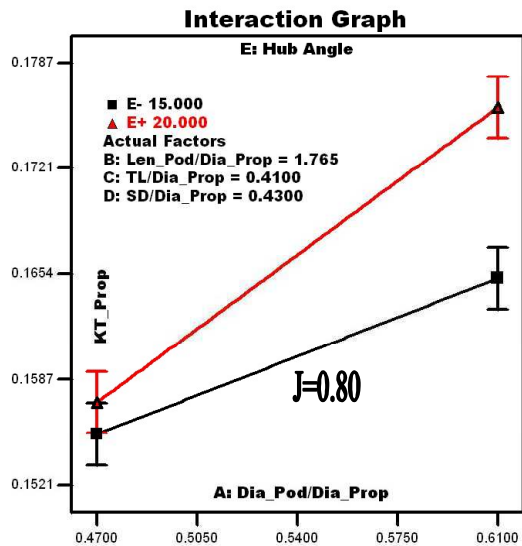


Fig. 19. DOE Analysis: The interaction effect of significant factors, D_{Pod}/D_{Prop} (A) and H_{Angle} (E) on propeller thrust at $J=0.8$ for puller propulsors.

S_{Dist}/D_{Prop} . At the low L_{Pod}/D_{Prop} value, the increase of S_{Dist}/D_{Prop} increased the K_{TUnit} , whereas at high L_{Pod}/D_{Prop} value, the increase of S_{Dist}/D_{Prop} decreased the K_{TUnit} . In other words, for the low S_{Dist}/D_{Prop} case, increasing L_{Pod}/D_{Prop} increased the K_{TUnit} , but for the high S_{Dist}/D_{Prop} case, increasing L_{Pod}/D_{Prop} decreased the K_{TUnit} .

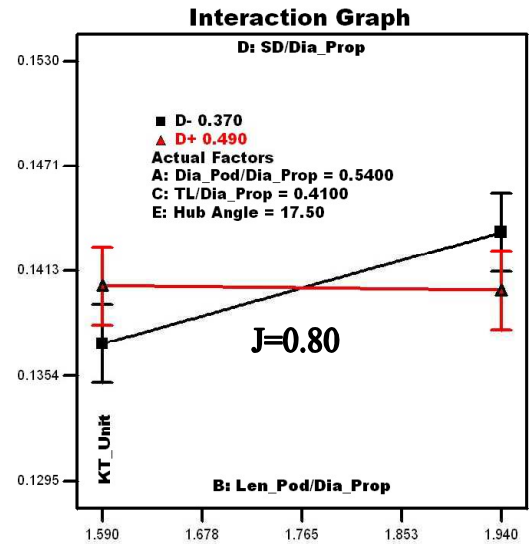


Fig. 20. DOE Analysis: The interaction effect of significant factors, L_{Pod}/D_{Prop} (B) and S_{Dist}/D_{Prop} (D) on unit thrust at $J=0.8$ for puller propulsors.

DOE Analysis of Pusher Propulsors

Table 5 lists all the factors and interactions of factors that have significant influence on the performance coefficients K_{TProp} , K_Q , η_{Prop} , K_{TUnit} and η_{Unit} for the pusher propulsors in the pod series. Table 5 shows that the significant factors that came up repeatedly over the range of J values were A (D_{Pod}/D_{Prop}), B (L_{Pod}/D_{Prop}), C (TL), D (S_{Dist}/D_{Prop}), E (H_{Angle}), AB (interaction of D_{Pod}/D_{Prop} and L_{Pod}/D_{Prop}) and BC (interaction of L_{Pod}/D_{Prop} and TL).

The factor H_{Angle} had significant impact on K_{TProp} , K_Q , η_{Prop} and η_{Unit} for all values of advance coefficient, whereas the factor A (D_{Pod}/D_{Prop}) had significant impact at moderate and high values of advance coefficient (in the range of $J=0.4\sim 1.1$). The factor B (L_{Pod}/D_{Prop}) had significant influence in the form of interaction with D (S_{Dist}/D_{Prop}) on K_{TUnit} at moderate values of J (in the range of $J=0.4\sim 0.7$) and as an individual factor at high values of J (in the range of $J=0.9\sim 1.1$). The factor D (S_{Dist}/D_{Prop}) appeared to have significant effect on K_{TProp} and η_{Prop} at advance coefficients of 0.8 and higher. The factor C (TL/D_{Prop}) had a noticeable impact on K_{TUnit} at low and moderate values of advance coefficient as shown in Table 5.

Fig. 20 shows the interaction effect BD (L_{Pod}/D_{Prop} and S_{Dist}/D_{Prop}) on K_{TUnit} at $J=0.8$; it shows that the effect of the factor L_{Pod}/D_{Prop} was opposite at the high and low values of

Table 5. Fractional factorial design results: List of significant factors and interaction of factors for pusher propulsors. Here, A is the ratio of pod diameter to propeller diameter, D_{Pod}/D_{Prop} , B is the ratio of pod length to propeller diameter, L_{Pod}/D_{Prop} , C is the ratio of pod taper length to propeller diameter, TL/D_{Prop} , D is the ratio of strut distance to propeller diameter, S_{Dist}/D_{Prop} , and E is the propeller hub taper angle, H_{Angle} .

Significant factor and interaction of factors										
J	K_{TProp}		K_{TUnit}		K_Q	η_{Prop}		η_{Unit}		
0.00	E	BC	C	AB	E	-	-	-	-	
0.10	E	BC	C	AB	E	E		E	AB	
0.20	E	BC	C	AB	E	E		E	AB	
0.30	E		C	AB	E	E		A, E		
0.40	A, E		A, C	BD	E	A, E		A, E		
0.50	A, E		A, C	BD	A, E	A, E		A, E		
0.60	A, E		A, C	BD	A, E	A, E		A, E		
0.70	A, E		A, C	BD	A, E	A, E		A, E		
0.80	A, D, E		A, C		A, E	A, D, E		A, E		
0.90	A, D, E		B, C		A, E	A, D, E		A, E		
1.00	A, D, E		B		A, E	A, D, E		A, D, E		
1.10	A, E		B		A, E	A, D, E		A, D, E		

Fig. 21 shows the effect of the factor D_{Pod}/D_{Prop} on K_{TProp} at $J=0.8$. For a fixed propeller diameter, as the pod diameter increased the K_{TProp} increased. The larger pod diameter created larger blockage to the flow in front of the propeller. The blockage in the flow reduced the local flow velocity, thus the propeller operated at lower effective advance coefficient, which resulted in an increase in K_{TProp} . The parameter, D_{Pod}/D_{Prop} had similar effect on K_{TProp} , K_Q , η_{Prop} and η_{Unit} for the other advance coefficient values shown in Table 5. Fig. 22 shows the effect of the factor D_{Pod}/D_{Prop} on K_{TUnit} at $J=0.8$. For a fixed propeller diameter, as the pod diameter increased the K_{TUnit} decreased. A larger pod diameter means higher drag on the pod, along with a larger blockage effect, which resulted in lower unit thrust.

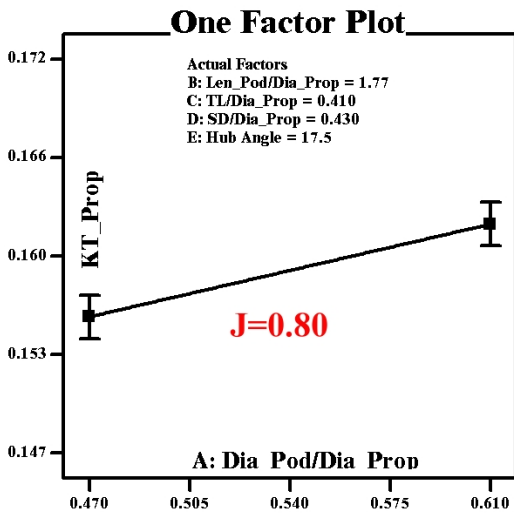


Fig. 21. DOE Analysis: The effect of D_{Pod}/D_{Prop} (A) on propeller thrust at $J=0.8$ for pusher propulsors.

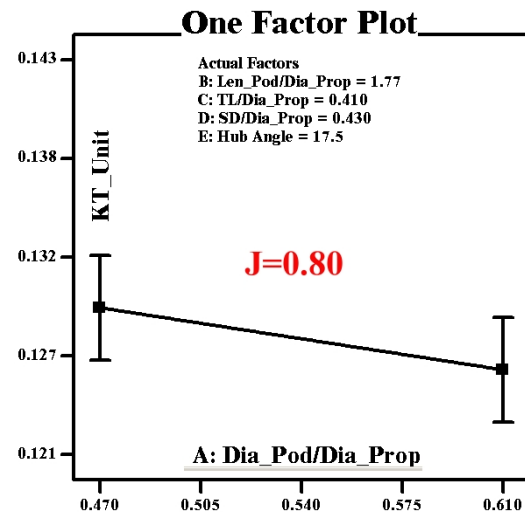


Fig. 22. DOE Analysis: The effect of D_{Pod}/D_{Prop} (A) on unit thrust at $J=0.8$ for pusher propulsors.

Fig. 23 shows the effect of the factor taper length, C (TL/D_{Prop}) on K_{TUnit} at $J=0.8$. For a fixed propeller diameter, as the pod taper length increased the K_{TUnit} increased. Taper length showed a similar effect on unit thrust at other advance coefficients but it did not have significant effect on K_{TProp} , K_Q , η_{Prop} and η_{Unit} at any of the advance coefficients.

Fig. 24 shows the effect of the strut distance, D (S_{Dist}/D_{Prop}) on propeller thrust; it shows that at $J=0.8$, as the strut distance increased, the K_{TProp} tended to decrease slightly because of blockage effect of the strut. The factor, S_{Dist}/D_{Prop} showed similar effect on η_{Prop} and η_{Unit} at high advance coefficients but did not show any effect on K_{TUnit} and K_Q at any advance coefficients.

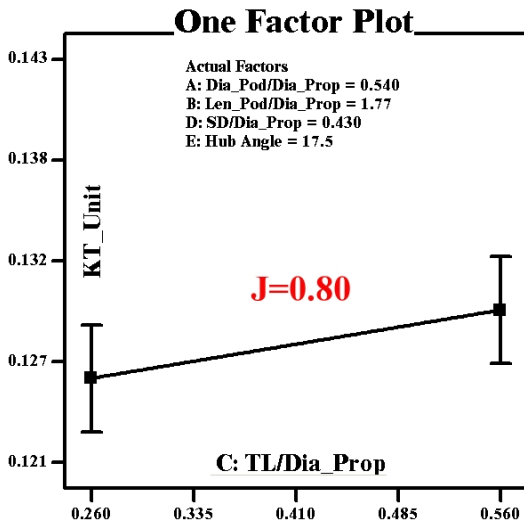


Fig. 23. DOE Analysis: The effect of TL/D_{Prop} (C) on unit thrust at $J=0.8$ for pusher propulsors.

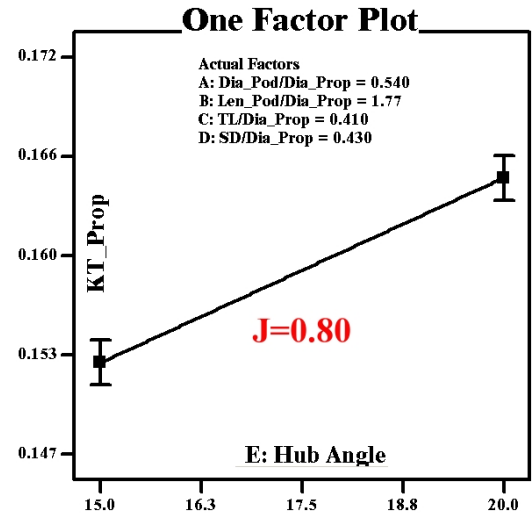


Fig. 25. DOE Analysis: The effect of H_{Angle} (E) on propeller thrust at $J=0.8$ for pusher propulsors.

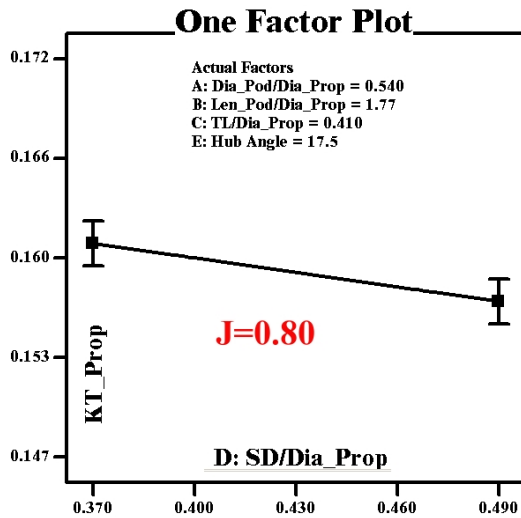


Fig. 24. DOE Analysis: The effect of S_{Dist}/D_{Prop} (D) on propeller thrust at $J=0.8$ for pusher propulsors.

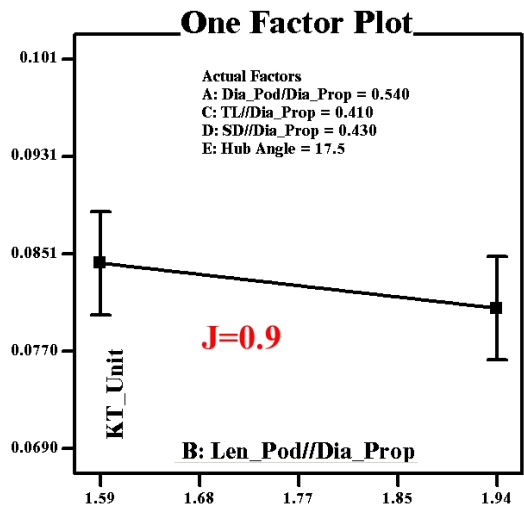


Fig. 26. DOE Analysis: The effect of L_{Pod}/D_{Prop} (B) on unit thrust at $J=0.9$ for pusher propulsors.

Fig. 25 shows the effect of hub angle, H_{Angle} on K_{TProp} at $J=0.8$. As the hub angle increased, the K_{TProp} also increased. The parameter, H_{Angle} had a similar effect on K_{TProp} , K_Q , η_{Prop} and η_{Unit} for the other advance coefficient values as shown in Table 5 but did not have any effect on K_{TUnit} at any advance coefficients. Fig. 26 shows the effect of pod length, L_{Pod}/D_{Prop} on K_{TUnit} at $J=0.9$. As the pod length increased, the K_{TUnit} decreased meaning longer pods had lower unit thrust. The parameter L_{Pod}/D_{Prop} showed a similar effect on only unit thrust at higher advance coefficients (J greater than 0.9).

The interaction of factors B and C, i.e. BC, (L_{Pod}/D_{Prop} and TL/D_{Prop}) had noticeable effect on K_{TProp} when J was equal to 0.3 or less. Fig. 27 shows that for constant propeller diameter, at $J=0$ and at lower taper length, increasing pod length resulted in lower propeller thrust, whereas at higher taper length, increasing pod length resulted in higher propeller thrust.

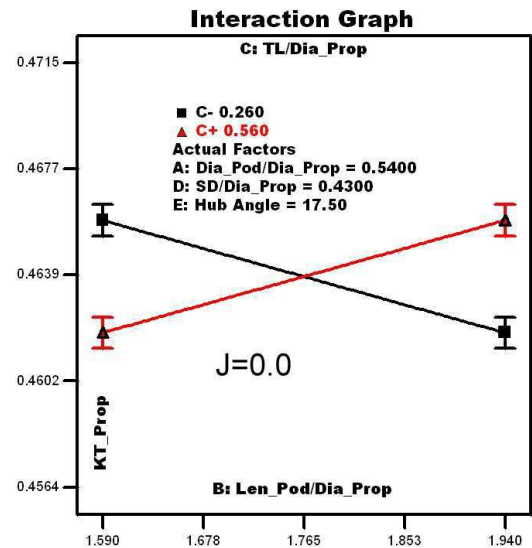


Fig. 27. DOE Analysis: The interaction effect of L_{Pod}/D_{Prop} (B) and TL/D_{Prop} (C) on propeller thrust at $J=0$ for pusher propulsors.

Fig. 28 shows the interaction effect of AB (D_{Pod}/D_{Prop} and L_{Pod}/D_{Prop}) on unit thrust at $J=0$. It shows that for constant propeller diameter, at lower pod diameter, increasing pod length resulted in an increase in unit thrust, whereas at higher pod diameter, increasing pod length produced a lower unit thrust. A similar effect was found in the range of $J=0$ to 0.4.

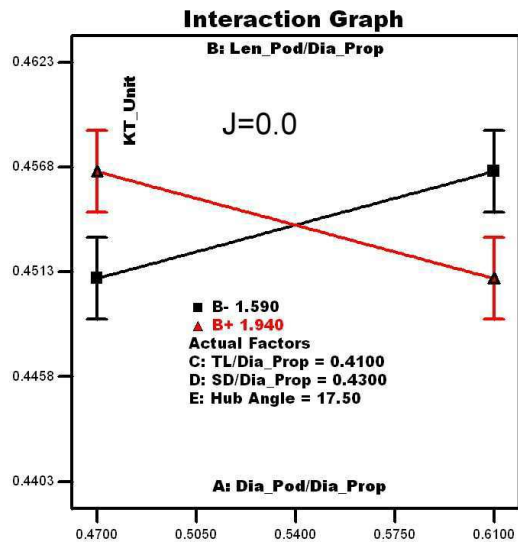


Fig. 28. DOE Analysis: The interaction effect of D_{Pod}/D_{Prop} (A) and L_{Pod}/D_{Prop} (B) on unit thrust at $J=0$ for pusher propulsors.

CONCLUDING REMARKS

A series of 16 pods were designed using a fractional factorial design technique to study the effects of five geometric parameters (pod diameter, pod length, pod taper length, strut distance and propeller hub angle) of podded propulsors in pusher and puller configurations. The experimental data on the pod series was acquired using a custom-designed pod testing system at the OERC towing tank at Memorial University. The findings of the analysis can be summarized as follows:

For a fixed propeller diameter, as the pod diameter increased, the propeller thrust, torque and efficiency increased for both puller and pusher propulsors; this might be attributed to the blockage effect of the pod. However, the increase in pod diameter resulted in a decrease in unit thrust for the pusher propulsors.

Pod length did not show an obvious effect on the performance coefficients of the puller propulsors, but it showed some effect on unit thrust coefficient of the pusher propulsors at higher advance coefficient regions. At advance coefficients of 0.9 or higher, for a fixed propeller diameter, as the pod length increased the propulsor unit thrust coefficient decreased, meaning that longer pods had lower unit thrust in the pusher configuration.

For the puller propulsors, as the hub taper angle increased, both propeller and propulsor unit thrust coefficients and efficiencies increased for all ranges of advance coefficients; this was more pronounced at low advance coefficients. However, hub angle had opposite effects on torque coefficients at low and high

advance coefficients. The torque increased with increasing taper angle at advance coefficients of 0.7 or lower but decreased at higher advance coefficients. For the pusher propulsors, as the hub taper angle increased, propeller and unit thrusts and propeller torque coefficients and efficiencies increased for all ranges of advance coefficients

The ratio of strut distance to propeller diameter had moderate effects on propeller thrust and torque coefficients for puller propulsors at moderate advance coefficients but only on propeller thrust for pusher propulsors. As the distance of the strut leading edge from the propeller plane increased, the propeller thrust and torque coefficient decreased.

Taper length of the pod aft end, the end away from the propeller, did not have a significant influence on performance of the puller propulsors within the range tested. However, it had significant effect on unit thrust of the pusher propulsors at all advance coefficients. For a fixed propeller diameter, as the pod taper length increased, the unit thrust also increased due to less pod drag on pods with high taper length.

The interaction of the factors pod diameter and hub angle had significant effect on both propeller and unit thrust and torque coefficients at moderate advance coefficient for the puller propulsors. For a fat pod, the influence of increased hub taper angle, which causes an increase in propeller and unit thrust coefficients, was more pronounced. The interaction of the factors showed little or no effect for the pusher propulsors.

For the pusher propulsors, the interaction of the factors pod length and pod taper length had noticeable effect on propeller thrust for low advance coefficients. When the ratio of the pod taper length to propeller diameter was low, increasing pod length resulted in lower propeller thrust, whereas at higher taper length increasing pod length resulted in higher propeller thrust.

For the pusher propulsors, the interaction effect of pod diameter and pod length was significant on unit thrust coefficient at low advance coefficients. The analysis showed that for a slender pod (low value of pod diameter to propeller diameter), increasing pod length resulted in an increase in unit thrust, whereas the opposite is true for the pod with a high value of the ratio of pod diameter to propeller diameter.

For the puller propulsors, the interaction effect pod length and strut distance was significant on unit thrust coefficient at moderate advance coefficients. The analysis showed that the impact of pod length was opposite at high and low values of strut distance. At the low pod length value, the increase of strut distance increased the unit thrust, whereas at high pod length value, the increase of strut distance decreased the unit thrust.

The measurement showed that there were significant variations in the propeller thrust, torque, unit thrust and propeller and unit efficiencies values due to the variations of the geometric parameters of the pods. The uncertainty analysis of the measurements showed that the level of uncertainty was within acceptable limits. The variations of the performance coefficients due to the geometry variations were outside of the errors, which

implied that the results were significant.

ACKNOWLEDGEMENTS

The authors thank the Natural Sciences and Engineering Research Council (NSERC) Canada, the National Research Council (NRC), Oceanic Consulting Corp., Thordon Bearings Inc., and Memorial University for their financial and other support. Thanks are also extended to Andrew MacNeill of Oceanic Consulting Corporation and Memorial University Technical Services Staff.

REFERENCES

- BOSE, N. and LUZNIK, L. "1996 Uncertainty Analysis in Propeller Open Water Tests." Intl Shipbuilding Progress, Vol. 43, no. 435, pp. 237-246.
- COLEMAN, H W. and STEELE, W. G. "1989 Experimentation and Uncertainty Analysis for Engineers." Wiley Interscience, 1989.
- DESIGN EXPERT, Version 6, Stat Ease, www.statease.com, 2005.
- GOUBAULT, P. and PÉRRÉE, J. "2004 Parametric investigations designed to help focused pod technology development." Proceedings of the 1st International Conference on Technological Advances in Podded Propulsion, Newcastle University, pp 27-28, UK, April 2004.
- HE, M., VEITCH B., BOSE N., BRUCE C. and LIU P. "2005a Numerical Simulations of Propeller Wake Impacting on a Strut." Proceedings of the CFD2005, St John's, NL Canada, 8p, August 2005.
- HE, M., VEITCH B., BOSE N. and LIU P. "2005b An Investigation on Wake/Strut Interaction of a Tractor-Type Podded Propulsor." Proceedings of the 7th CMHSC, Halifax, NS Canada, 8p, September 2005.
- HESS, D.E., NIGON, R.T., BEDEL, J.W. "2000 Dynamometer Calibration and Usage." Research and Development Report No. NSWCCD-50-TR-2000/040, Hydromechanics Directorate, Carderrock Division, Naval Surface Warfare Center, West Bethesda, Maryland, 31p.
- ISLAM, M. F. "2004 Numerical investigation on effects of hub taper angle and Pod-strut geometry on propulsive performance of pusher Propeller configurations." Master of Engineering thesis, Memorial University of Newfoundland, Canada, 136 p.
- ISLAM, M. F., TAYLOR, R., QUINTON J., VEITCH, B., BOSE, N., COLBOURNE, B. and LIU, P. "2004 Numerical investigation of propulsive characteristics of podded propeller." Proceedings of the 1st International Conference on Technological Advances in Podded Propulsion, Newcastle University, UK, pp. 513-525, April 2004.
- ISLAM, M., VEITCH, B., BOSE, N. and LIU, P. "2005 Cavitation Characteristics of Pushing and Pulling Podded Propellers With Different Hub Taper Angles." Proceedings. of the 7th CMHSC, Halifax, NS Canada, 7p, September 2005 .
- ISLAM, M. F. "2006 Experimental Results: Open Water Performance of Puller Podded Propulsors with Varied Geometry." Ocean Engineering Research Center (OERC) Report No. OERC-2006-02, St. John's, NL, Canada, 109p, 2006.
- ISLAM, M. F. "2006a Calibration and Usages of NSERC-NRC Pod Dynamometer System." Ocean Engineering Research Center (OERC) Report No. OERC-2006-04, St. John's, NL, Canada, 86p, 2006.
- ISLAM, M. F. "2006b Uncertainty analysis of NSERC-NRC pod dynamometer system." Ocean Engineering Research Center (OERC) Report No. OERC-2006-05, St. John's, NL, Canada, 96p, 2006.
- ISLAM, M. "2004 A proposal for Doctoral research in the Faculty of Engineering and Applied Science." Engineering and Applied Science, Memorial University of Newfoundland, 85p.
- ISLAM, M. F., VEITCH, B., BOSE, N. and LIU, P. "2006 Hydrodynamic characteristics of pod propeller units of highly tapered hub." Proceedings, Propellers/Shafting, Society of Naval Architects and Marine Engineers, Virginia Beach, USA, 12p, September 2006.
- ITTC - Recommended Procedures, "2002a Propulsion, Performance - Podded Propeller Tests and Extrapolation" 7.5-02-03-01.3, Revision 00, 9p.
- ITTC - Recommended Procedures, Propulsion, "2002b Propulsor Uncertainty Analysis, Example for Open Water Test." 7.5-02-03-02.2, Revision 00, 2002.
- KARAFIATH, G. and LYONS, D. "1998 Hydrodynamic performance with Pod Propulsion - U.S. Navy experience." American Towing Tank Conference, Iowa City, 23p, 1998.
- LIU, P. "2006 The Design of a Podded Propeller Base Model Geometry and Prediction of Its hydrodynamics." Technical Report no. TR-2006-16, Institute for Ocean Technology, National Research Council Canada, 16 p,
- MACNEILL, A., TAYLOR, R., MOLLOY, S., BOSE, N., VEITCH, B., RANDELL, T. and LIU, P. "2004 Design of model pod test unit, Proceedings of the 1st International Conference on Technological Advances in Podded Propulsion." Newcastle University, UK, pp. 447-458, April 2004.
- MEWIS, F. "2001 The efficiency of pod propulsion." HADMAR 2001, Bulgaria, October, 7p, 2001.
- MOLLOY, S., ISLAM, M. F., HE, M., VEITCH, B., BOSE, N., WANG J., AKINTURK, A. and LIU, P., "2005 Use of factorial design in podded propulsors geometric series." Proceedings of the 7th CMHSC, Halifax, NS Canada, 8 p, September 2005.
- MOLLOY S. "2003 A proposal for Doctoral research in the Faculty of Engineering and Applied Science." Engineering and Applied Science, Memorial University of Newfoundland, 86p.
- MONTGOMERY, D.C. "2005 Design and analysis of experiments." sixth Edition, Wiley & Sons, USA, 189p, 2005.
- TAYLOR, R. VEITCH, B. and BOSE, N. "2005 The Influence of Hub Taper Angle on Podded Propeller Performance: 'Propeller Only' Tests vs. 'Podded Propeller Unit' Tests." Proceedings of the 7th CMHSC, Halifax, NS Canada, 8p, September 2005.
- TAYLOR R. "2005 Experimental Investigation of the Influence of Hub Taper Angle on the Performance of Push and Pull Configuration Podded Propellers." Master's of Engineering Thesis, Memorial University of Newfoundland, Canada, 120p, 2005.

APPENDIX

Table A-1. Puller Configuration: Propeller Thrust Coefficient, K_{Tprop}

J	Pod 01	Pod 02	Pod 03	Pod 04	Pod 05	Pod 06	Pod 07	Pod 08	Pod 09	Pod 10	Pod 11	Pod 12	Pod 13	Pod 14	Pod 15	Pod 16
0.00	0.4688	0.4865	0.4693	0.4850	0.4833	0.4691	0.4689	0.4826	0.4763	0.4900	0.4924	0.4721	0.4903	0.4719	0.4642	0.4950
0.10	0.4425	0.4542	0.4410	0.4549	0.4556	0.4430	0.4430	0.4544	0.4490	0.4615	0.4638	0.4436	0.4617	0.4448	0.4424	0.4640
0.20	0.4048	0.4179	0.4038	0.4174	0.4179	0.4044	0.4041	0.4157	0.4092	0.4200	0.4260	0.4052	0.4260	0.4054	0.4055	0.4267
0.30	0.3663	0.3782	0.3636	0.3731	0.3777	0.3640	0.3666	0.3741	0.3723	0.3857	0.3860	0.3688	0.3885	0.3689	0.3675	0.3867
0.40	0.3308	0.3327	0.3230	0.3290	0.3363	0.3246	0.3281	0.3330	0.3311	0.3440	0.3481	0.3269	0.3507	0.3274	0.3321	0.3410
0.50	0.2825	0.2858	0.2807	0.2874	0.2906	0.2788	0.2822	0.2902	0.2881	0.3013	0.3059	0.2839	0.3083	0.2828	0.2829	0.2999
0.60	0.2403	0.2432	0.2386	0.2439	0.2448	0.2378	0.2400	0.2422	0.2483	0.2565	0.2601	0.2420	0.2601	0.2435	0.2466	0.2604
0.65	0.2179	0.2200	0.2162	0.2189	0.2266	0.2146	0.2192	0.2194	0.2268	0.2341	0.2374	0.2230	0.2408	0.2265	0.2227	0.2403
0.70	0.2022	0.2004	0.1945	0.2023	0.2045	0.1941	0.1994	0.2000	0.2067	0.2153	0.2149	0.2007	0.2201	0.2071	0.2041	0.2193
0.75	0.1773	0.1776	0.1765	0.1792	0.1795	0.1733	0.1796	0.1787	0.1899	0.1907	0.1966	0.1817	0.1954	0.1831	0.1834	0.1966
0.80	0.1587	0.1579	0.1521	0.1553	0.1616	0.1549	0.1581	0.1551	0.1683	0.1729	0.1760	0.1631	0.1786	0.1657	0.1649	0.1787
0.85	0.1376	0.1365	0.1334	0.1395	0.1379	0.1339	0.1379	0.1348	0.1472	0.1481	0.1529	0.1411	0.1548	0.1422	0.1429	0.1549
0.90	0.1130	0.1166	0.1129	0.1136	0.1139	0.1102	0.1139	0.1134	0.1230	0.1271	0.1341	0.1187	0.1368	0.1231	0.1243	0.1344
0.95	0.0946	0.0922	0.0883	0.0916	0.0933	0.0909	0.0942	0.0916	0.1057	0.1090	0.1097	0.0999	0.1115	0.1025	0.1046	0.1138
1.00	0.0720	0.0662	0.0652	0.0671	0.0644	0.0684	0.0697	0.0666	0.0833	0.0871	0.0845	0.0762	0.0906	0.0816	0.0801	0.0890
1.10	0.0262	0.0168	0.0205	0.0170	0.0186	0.0207	0.0242	0.0197	0.0332	0.0379	0.0409	0.0310	0.0468	0.0384	0.0356	0.0447
1.20	-0.0299	-0.0233	-0.0371	-0.0228	-0.0201	-0.0291	-0.0294	-0.0209	-0.0120	-0.0070	-0.0049	-0.0163	-0.0015	-0.0101	-0.0145	-0.0084

Table A-2. Puller Configuration: Propeller Torque Coefficient, $10K_Q$

J	Pod 01	Pod 02	Pod 03	Pod 04	Pod 05	Pod 06	Pod 07	Pod 08	Pod 09	Pod 10	Pod 11	Pod 12	Pod 13	Pod 14	Pod 15	Pod 16
0.00	0.6698	0.6828	0.6798	0.6806	0.6848	0.6856	0.6829	0.6815	0.6808	0.6891	0.6921	0.6830	0.6916	0.6825	0.6795	0.6854
0.10	0.6367	0.6444	0.6462	0.6480	0.6443	0.6471	0.6446	0.6440	0.6492	0.6497	0.6511	0.6433	0.6511	0.6454	0.6453	0.6515
0.20	0.5972	0.5991	0.6037	0.6049	0.6008	0.6054	0.6025	0.6002	0.6082	0.6019	0.6078	0.6038	0.6092	0.6057	0.6067	0.6077
0.30	0.5564	0.5519	0.5601	0.5571	0.5559	0.5625	0.5621	0.5520	0.5669	0.5638	0.5625	0.5635	0.5667	0.5648	0.5656	0.5653
0.40	0.5066	0.4986	0.5099	0.4991	0.4982	0.5123	0.5126	0.4986	0.5120	0.5062	0.5122	0.5136	0.5124	0.5102	0.5192	0.5155
0.50	0.4587	0.4460	0.4633	0.4510	0.4445	0.4568	0.4591	0.4491	0.4662	0.4602	0.4655	0.4656	0.4643	0.4623	0.4659	0.4677
0.60	0.4018	0.3954	0.4112	0.3949	0.3988	0.4076	0.4088	0.3955	0.4184	0.4103	0.4110	0.4079	0.4152	0.4123	0.4177	0.4109
0.65	0.3772	0.3645	0.3789	0.3656	0.3679	0.3787	0.3796	0.3629	0.3898	0.3772	0.3835	0.3844	0.3873	0.3909	0.3897	0.3832
0.70	0.3534	0.3374	0.3506	0.3368	0.3391	0.3533	0.3548	0.3387	0.3630	0.3525	0.3561	0.3538	0.3605	0.3643	0.3645	0.3572
0.75	0.3221	0.3089	0.3272	0.3107	0.3095	0.3186	0.3249	0.3091	0.3336	0.3261	0.3325	0.3288	0.3288	0.3341	0.3346	0.3268
0.80	0.2955	0.2767	0.2993	0.2745	0.2802	0.2960	0.3000	0.2760	0.3101	0.2974	0.3024	0.3038	0.3063	0.3093	0.3121	0.3021
0.85	0.2656	0.2495	0.2689	0.2484	0.2515	0.2661	0.2705	0.2462	0.2816	0.2655	0.2653	0.2766	0.2741	0.2774	0.2798	0.2698
0.90	0.2330	0.2142	0.2342	0.2146	0.2145	0.2306	0.2344	0.2129	0.2464	0.2299	0.2363	0.2417	0.2442	0.2494	0.2508	0.2396
0.95	0.2032	0.1802	0.2002	0.1835	0.1852	0.2013	0.2059	0.1804	0.2221	0.1997	0.2074	0.2123	0.2104	0.2190	0.2213	0.2089
1.00	0.1678	0.1461	0.1660	0.1481	0.1468	0.1672	0.1708	0.1438	0.1895	0.1727	0.1701	0.1783	0.1772	0.1885	0.1845	0.1719
1.10	0.0947	0.0699	0.0923	0.0708	0.0761	0.0881	0.0916	0.0715	0.1078	0.0994	0.1036	0.1060	0.1118	0.1142	0.1119	0.1046
1.20	-0.0053	-0.0208	-0.0100	-0.0159	-0.0171	0.0042	0.0057	-0.0155	0.0317	0.0213	0.0244	0.0230	0.0322	0.0310	0.0258	0.0183

Table A-3. Puller Configuration: Propulsor (Unit) Thrust Coefficient, K_{Tunit}

J	Pod 01	Pod 02	Pod 03	Pod 04	Pod 05	Pod 06	Pod 07	Pod 08	Pod 09	Pod 10	Pod 11	Pod 12	Pod 13	Pod 14	Pod 15	Pod 16
0.00	0.4620	0.4836	0.4632	0.4780	0.4707	0.4622	0.4576	0.4685	0.4659	0.4792	0.4788	0.4607	0.4760	0.4611	0.4577	0.4840
0.10	0.4307	0.4450	0.4289	0.4439	0.4431	0.4353	0.4322	0.4319	0.4351	0.4450	0.4479	0.4342	0.4453	0.4300	0.4305	0.4499
0.20	0.3841	0.4085	0.3926	0.4040	0.4060	0.3934	0.3932	0.3945	0.3892	0.4067	0.4102	0.3895	0.4075	0.3880	0.3924	0.4095
0.30	0.3407	0.3647	0.3497	0.3525	0.3646	0.3495	0.3560	0.3537	0.3487	0.3693	0.3709	0.3516	0.3666	0.3467	0.3528	0.3670
0.40	0.3032	0.3208	0.3092	0.3135	0.3188	0.3063	0.3151	0.3158	0.3094	0.3273	0.3301	0.3099	0.3236	0.3058	0.3163	0.3281
0.50	0.2645	0.2674	0.2624	0.2699	0.2742	0.2634	0.2696	0.2715	0.2660	0.2798	0.2833	0.2685	0.2801	0.2637	0.2677	0.2849
0.60	0.2212	0.2248	0.2233	0.2201	0.2274	0.2183	0.2295	0.2261	0.2234	0.2373	0.2365	0.2229	0.2376	0.2204	0.2262	0.2406
0.65	0.1866	0.1969	0.2003	0.1972	0.2067	0.1972	0.2035	0.2050	0.2010	0.2125	0.2171	0.2040	0.2122	0.2019	0.2028	0.2182
0.70	0.1735	0.1761	0.1767	0.1786	0.1822	0.1735	0.1833	0.1825	0.1779	0.1904	0.1956	0.1833	0.1943	0.1832	0.1867	0.1974
0.75	0.1522	0.1530	0.1585	0.1506	0.1630	0.1548	0.1629	0.1595	0.1581	0.1668	0.1711	0.1596	0.1701	0.1618	0.1658	0.1732
0.80	0.1351	0.1307	0.1385	0.1295	0.1419	0.1330	0.1386	0.1350	0.1375	0.1475	0.1530	0.1415	0.1507	0.1410	0.1460	0.1511
0.85	0.1126	0.1115	0.1130	0.1107	0.1176	0.1164	0.1178	0.1120	0.1173	0.1212	0.1311	0.1188	0.1291	0.1216	0.1236	0.1282
0.90	0.0884	0.0839	0.0931	0.0884	0.0969	0.0934	0.0931	0.0870	0.0941	0.1017	0.1072	0.0980	0.1081	0.0997	0.1001	0.1046
0.95	0.0762	0.0633	0.0647	0.0639	0.0763	0.0684	0.0685	0.0696	0.0726	0.0780	0.0791	0.0790	0.0847	0.0814	0.0769	0.0857
1.00	0.0466	0.0401	0.0454	0.0395	0.0514	0.0489	0.0393	0.0433	0.0509	0.0566	0.0544	0.0542	0.0630	0.0547	0.0505	0.0594
1.10	-0.0013	-0.0104	-0.0077	-0.0018	0.0014	-0.0051	-0.0023	0.0012	0.0038	0.0115	0.0084	0.0086	0.0183	0.0072	0.0076	0.0153
1.20	-0.0612	-0.0500	-0.0719	-0.0457	-0.0413	-0.0572	-0.0619	-0.0503	-0.0525	-0.0435	-0.0501	-0.0400	-0.0309	-0.0466	-0.0458	-0.0409

Table A-4. Pusher Configuration: Propeller Thrust Coefficient, K_{Tprop}

J	Pod 01	Pod 02	Pod 03	Pod 04	Pod 05	Pod 06	Pod 07	Pod 08	Pod 09	Pod 10	Pod 11	Pod 12	Pod 13	Pod 14	Pod 15	Pod 16
0.00	0.4655	0.4681	0.4598	0.4638	0.4643	0.4564	0.4641	0.4715	0.4605	0.4712	0.4667	0.4576	0.4672	0.4601	0.4595	0.4660
0.10	0.4354	0.4408	0.4302	0.4356	0.4392	0.4267	0.4328	0.4429	0.4327	0.4445	0.4393	0.4322	0.4371	0.4335	0.4317	0.4390
0.20	0.4038	0.4019	0.3978	0.3975	0.4059	0.3924	0.3936	0.4116	0.3968	0.4119	0.4095	0.3960	0.4054	0.3949	0.3962	0.4029
0.30	0.3618	0.3667	0.3566	0.3616	0.3654	0.3571	0.3574	0.3733	0.3665	0.3692	0.3685	0.3609	0.3731	0.3586	0.3579	0.3632
0.40	0.3210	0.3283	0.3213	0.3264	0.3288	0.3213	0.3186	0.3271	0.3203	0.3347	0.3343	0.3200	0.3320	0.3239	0.3208	0.3334
0.50	0.2745	0.2838	0.2740	0.2855	0.2867	0.2728	0.2778	0.2871	0.2767	0.2914	0.2934	0.2741	0.2855	0.2842	0.2770	0.2877
0.60	0.2329	0.2415	0.2358	0.2416	0.2435	0.2297	0.2371	0.2438	0.2378	0.2481	0.2500	0.2357	0.2465	0.2393	0.2332	0.2478
0.65	0.2101	0.2223	0.2108	0.2216	0.2261	0.2073	0.2136	0.2198	0.2162	0.2302	0.2291	0.2135	0.2295	0.2168	0.2159	0.2276
0.70	0.1921	0.2012	0.1921	0.2006	0.2042	0.1923	0.1971	0.2018	0.1974	0.2103	0.2060	0.1960	0.2112	0.1956	0.1974	0.2102
0.75	0.1710	0.1801	0.1708	0.1786	0.1830	0.1695	0.1755	0.1833	0.1782	0.1909	0.1860	0.1740	0.1926	0.1741	0.1766	0.1892
0.80	0.1511	0.1587	0.1469	0.1600	0.1634	0.1497	0.1571	0.1600	0.1561	0.1695	0.1670	0.1549	0.1724	0.1523	0.1571	0.1660
0.85	0.1317	0.1405	0.1269	0.1413	0.1433	0.1261	0.1334	0.1431	0.1359	0.1487	0.1464	0.1330	0.1508	0.1339	0.1369	0.1481
0.90	0.1133	0.1211	0.1033	0.1171	0.1191	0.1039	0.1123	0.1191	0.1122	0.1275	0.1274	0.1088	0.1312	0.1108	0.1120	0.1244
0.95	0.0892	0.0979	0.0881	0.0973	0.1009	0.0845	0.0932	0.1003	0.0943	0.1083	0.1054	0.0887	0.1108	0.0924	0.0958	0.1089
1.00	0.0644	0.0773	0.0602	0.0754	0.0776	0.0626	0.0700	0.0773	0.0730	0.0887	0.0870	0.0682	0.0911	0.0701	0.0730	0.0883
1.10	0.0102	0.0284	0.0160	0.0299	0.0352	0.0151	0.0229	0.0304	0.0275	0.0429	0.0428	0.0228	0.0518	0.0226	0.0285	0.0440
1.20	-0.0412	-0.0225	-0.0351	-0.0192	-0.0163	-0.0296	-0.0246	-0.0205	-0.0186	-0.0019	-0.0086	-0.0106	0.0017	-0.0199	-0.0176	-0.0020

Table A-5. Pusher Configuration: Propeller Torque Coefficient, $10K_Q$

J	Pod 01	Pod 02	Pod 03	Pod 04	Pod 05	Pod 06	Pod 07	Pod 08	Pod 09	Pod 10	Pod 11	Pod 12	Pod 13	Pod 14	Pod 15	Pod 16
0.00	0.6571	0.6552	0.6579	0.6818	0.6852	0.6588	0.6609	0.6832	0.6585	0.6790	0.6834	0.6578	0.6828	0.6656	0.6532	0.6740
0.10	0.6188	0.6349	0.6268	0.6311	0.6314	0.6220	0.6240	0.6421	0.6324	0.6421	0.6343	0.6243	0.6322	0.6373	0.6269	0.6316
0.20	0.5789	0.5925	0.5871	0.5853	0.5956	0.5812	0.5808	0.6048	0.5891	0.6054	0.5956	0.5834	0.5964	0.5903	0.5872	0.5981
0.30	0.5311	0.5380	0.5424	0.5420	0.5445	0.5361	0.5344	0.5619	0.5509	0.5568	0.5470	0.5383	0.5550	0.5494	0.5407	0.5528
0.40	0.4828	0.4978	0.4920	0.5071	0.4996	0.4981	0.4836	0.5072	0.4927	0.5168	0.5064	0.4941	0.5044	0.4931	0.4890	0.5077
0.50	0.4304	0.4487	0.4360	0.4570	0.4507	0.4342	0.4441	0.4612	0.4386	0.4581	0.4619	0.4319	0.4543	0.4494	0.4377	0.4611
0.60	0.3775	0.4014	0.3847	0.4013	0.3965	0.3832	0.3906	0.4139	0.3967	0.4089	0.4098	0.3837	0.4078	0.3903	0.3838	0.4071
0.65	0.3501	0.3734	0.3559	0.3740	0.3738	0.3490	0.3600	0.3823	0.3658	0.3911	0.3844	0.3573	0.3879	0.3649	0.3603	0.3882
0.70	0.3267	0.3468	0.3324	0.3512	0.3428	0.3292	0.3397	0.3537	0.3403	0.3656	0.3556	0.3329	0.3636	0.3356	0.3363	0.3650
0.75	0.2989	0.3188	0.3075	0.3232	0.3227	0.2988	0.3093	0.3319	0.3161	0.3380	0.3274	0.3073	0.3406	0.3067	0.3109	0.3355
0.80	0.2750	0.2949	0.2806	0.2984	0.3000	0.2765	0.2869	0.3027	0.2860	0.3094	0.2990	0.2856	0.3122	0.2806	0.2808	0.3099
0.85	0.2509	0.2647	0.2524	0.2731	0.2722	0.2487	0.2572	0.2851	0.2593	0.2850	0.2730	0.2627	0.2887	0.2566	0.2580	0.2908
0.90	0.2261	0.2408	0.2154	0.2451	0.2384	0.2189	0.2307	0.2504	0.2318	0.2577	0.2463	0.2338	0.2620	0.2285	0.2293	0.2626
0.95	0.1968	0.2106	0.1926	0.2247	0.2138	0.1896	0.2017	0.2292	0.2108	0.2300	0.2252	0.2106	0.2353	0.2042	0.2073	0.2349
1.00	0.1621	0.1752	0.1619	0.1933	0.1872	0.1574	0.1661	0.2002	0.1823	0.2055	0.2008	0.1869	0.2120	0.1736	0.1716	0.2084
1.10	0.0833	0.1189	0.1034	0.1295	0.1215	0.0935	0.1054	0.1352	0.1142	0.1441	0.1462	0.1224	0.1539	0.1108	0.1139	0.1566
1.20	-0.0097	0.0400	0.0149	0.0406	0.0478	0.0145	0.0213	0.0344	0.0379	0.0819	0.0731	0.0505	0.0887	0.0404	0.0391	0.0786

Table A-6. Pusher Configuration: Propulsor (Unit) Thrust Coefficient, K_{Tunit}

J	Pod 01	Pod 02	Pod 03	Pod 04	Pod 05	Pod 06	Pod 07	Pod 08	Pod 09	Pod 10	Pod 11	Pod 12	Pod 13	Pod 14	Pod 15	Pod 16
0.00	0.4403	0.4505	0.4583	0.4524	0.4502	0.4607	0.4617	0.4623	0.4582	0.4448	0.4537	0.4610	0.4497	0.4475	0.4560	0.4517
0.10	0.4031	0.4186	0.4238	0.4211	0.4213	0.4236	0.4260	0.4319	0.4262	0.4184	0.4176	0.4282	0.4114	0.4189	0.4203	0.4190
0.20	0.3725	0.3823	0.3912	0.3783	0.3859	0.3874	0.3883	0.3951	0.3856	0.3842	0.3801	0.3852	0.3737	0.3855	0.3829	0.3754
0.30	0.3347	0.3424	0.3494	0.3437	0.3396	0.3484	0.3463	0.3562	0.3444	0.3398	0.3381	0.3486	0.3422	0.3437	0.3424	0.3432
0.40	0.2953	0.3009	0.3058	0.3020	0.2987	0.3107	0.3050	0.3066	0.3004	0.2922	0.2989	0.3019	0.2964	0.3045	0.2999	0.3011
0.50	0.2553	0.2570	0.2592	0.2564	0.2521	0.2610	0.2651	0.2660	0.2605	0.2505	0.2541	0.2567	0.2478	0.2555	0.2520	0.2544
0.60	0.2134	0.2121	0.2181	0.2169	0.2090	0.2163	0.2255	0.2188	0.2140	0.2060	0.2127	0.2108	0.2036	0.2101	0.2101	0.2097
0.65	0.1924	0.1902	0.1940	0.1901	0.1887	0.1866	0.2041	0.2014	0.1875	0.1859	0.1915	0.1897	0.1864	0.1831	0.1836	0.1893
0.70	0.1712	0.1696	0.1687	0.1715	0.1702	0.1648	0.1844	0.1783	0.1682	0.1687	0.1714	0.1692	0.1672	0.1660	0.1644	0.1739
0.75	0.1489	0.1456	0.1505	0.1479	0.1449	0.1420	0.1635	0.1568	0.1469	0.1441	0.1493	0.1452	0.1420	0.1470	0.1407	0.1533
0.80	0.1328	0.1228	0.1241	0.1262	0.1257	0.1256	0.1429	0.1337	0.1250	0.1255	0.1297	0.1277	0.1261	0.1221	0.1214	0.1290
0.85	0.1136	0.1034	0.1077	0.1077	0.1039	0.0979	0.1203	0.1182	0.1069	0.1044	0.1102	0.1029	0.1031	0.1009	0.1022	0.1076
0.90	0.1011	0.0814	0.0830	0.0806	0.0778	0.0772	0.0881	0.0904	0.0808	0.0779	0.0909	0.0783	0.0804	0.0792	0.0690	0.0821
0.95	0.0714	0.0524	0.0584	0.0617	0.0583	0.0520	0.0652	0.0711	0.0588	0.0623	0.0666	0.0556	0.0582	0.0526	0.0511	0.0614
1.00	0.0423	0.0297	0.0255	0.0336	0.0377	0.0307	0.0421	0.0434	0.0327	0.0409	0.0446	0.0316	0.0416	0.0253	0.0312	0.0344
1.10	-0.0085	-0.0240	-0.0264	-0.0186	-0.0206	-0.0333	-0.0082	-0.0045	-0.0098	-0.0073	-0.0091	-0.0051	-0.0014	-0.0177	-0.0228	-0.0088
1.20	-0.0827	-0.0760	-0.0875	-0.0726	-0.0803	-0.0916	-0.0753	-0.0514	-0.0506	-0.0583	-0.0662	-0.0439	-0.0430	-0.0763	-0.0742	-0.0746